Requirement for *Pbx1* in skeletal patterning and programming chondrocyte proliferation and differentiation

Licia Selleri[1],*, Michael J. Depew[2], Yakop Jacobs[1], Sumit K. Chanda[1], Kwok Y. Tsang[3], Kathryn S. E. Cheah[3], John L. R. Rubenstein[2], Stephen O'Gorman[4] and Michael L. Cleary[1],*

[1]Department of Pathology, Stanford University School of Medicine, Stanford, CA 94305, 650-723-5471, USA
[2]Nina Ireland Laboratory of Developmental Neurobiology, University of California San Francisco, San Francisco, CA, USA
[3]Department of Biochemistry, The University of Hong Kong, Hong Kong, China
[4]Gene Expression Laboratory, The Salk Institute for Biological Studies, La Jolla, CA 92037, USA
*Authors for correspondence (e-mail: mcleary@stanford.edu or lselleri@cmgm.stanford.edu)

SUMMARY

Pbx1 and a subset of homeodomain proteins collaboratively bind DNA as higher-order molecular complexes with unknown consequences for mammalian development. Pbx1 contributions were investigated through characterization of *Pbx1*-deficient mice. *Pbx1* mutants died at embryonic day 15/16 with severe hypoplasia or aplasia of multiple organs and widespread patterning defects of the axial and appendicular skeleton. An obligatory role for *Pbx1* in limb axis patterning was apparent from malformations of proximal skeletal elements, but distal structures were unaffected. In addition to multiple rib and vertebral malformations, neural crest cell-derived skeletal structures of the second branchial arch were morphologically transformed into elements reminiscent of first arch-derived cartilages. Although the skeletal malformations did not phenocopy single or compound Hox gene defects, they were restricted to domains specified by Hox proteins bearing Pbx dimerization motifs and unaccompanied by alterations in Hox gene expression. In affected domains of limbs and ribs, chondrocyte proliferation was markedly diminished and there was a notable increase of hypertrophic chondrocytes, accompanied by premature ossification of bone. The pattern of expression of genes known to regulate chondrocyte differentiation was not perturbed in Pbx1-deficient cartilage at early days of embryonic skeletogenesis, however precocious expression of *Col1a1*, a marker of bone formation, was found. These studies demonstrate a role for Pbx1 in multiple developmental programs and reveal a novel function in co-ordinating the extent and/or timing of proliferation with terminal differentiation. This impacts on the rate of endochondral ossification and bone formation and suggests a mechanistic basis for most of the observed skeletal malformations.

Key words: Pbx1, Skeleton, Limb, Branchial arch homeosis, Hox, Chondrocyte proliferation, Mouse

INTRODUCTION

Pbx1 is a TALE (three amino acid loop extension) class homeodomain protein originally identified as the product of an oncogene in a subset of childhood leukemias (Nourse et al., 1990; Kamps et al., 1990). Subsequent studies have shown that Pbx1 is a homolog of *Drosophila* extradenticle (EXD) and a component of various protein complexes implicated in developmental gene expression (reviewed by Mann and Chan, 1996). The transcriptional activity of Pbx1 is regulated in part by nuclear import mediated by dimerization with other TALE class homeodomain proteins such as Meis/Prep1 (Berthelsen et al., 1999). The latter are evolutionarily related to but distinct from Pbx proteins (Burglin, 1997; Chen et al., 1997; Moscow et al., 1995), with which they form stable, nuclear DNA-binding complexes (Bischof et al., 1998; Chang et al., 1997; Knoepfler et al., 1997; Berthelsen et al., 1998a; Berthelsen et al., 1999). Biochemical analyses suggest that heterodimers of Pbx and Meis-related proteins contribute to the regulation of several genes (Berthelsen et al., 1998; Berthelsen et al., 1999; Bischof et al., 1998; Swift et al., 1998) in different tissues.

As a TALE heterodimer, Pbx displays an ability to simultaneously interact and bind DNA with Hox proteins thereby forming trimeric complexes on appropriate DNA sites (Berthelsen et al., 1998; Jacobs et al., 1999; Schnabel et al., 2000). Furthermore, two essential Hoxb1 hindbrain enhancers contain DNA binding sites that support the in vitro assembly of trimeric Hox-TALE complexes and are necessary for hindbrain enhancer activity in vivo (Jacobs et al., 1999; Ferretti et al., 2000). Numerous studies have demonstrated that interactions with Pbx1 result in enhanced Hox DNA binding affinities and specificities in vitro (Chan et al., 1994; Chang et al., 1995; Chang et al., 1996; Knoepfler and Kamps, 1995; Lu et al., 1995; Peers et al., 1995; Peltenberg and Murre, 1996; Phelan et al., 1995; Shen et al., 1996; van Dijk and Murre, 1994). These interactions are confined to a subset of Hox and other homeodomain proteins that contain characteristic tryptophan-bearing dimerization motifs. Genetic analyses in

both mice and *Drosophila* provide in vivo support that Pbx and EXD (Peifer and Weischaus, 1990; Rauskolb et al., 1993) function in concert with Hox proteins during development through response elements containing their cognate DNA binding sites (Chan et al., 1994; Maconochie et al., 1997; Popperl et al., 1995). Thus, Pbx proteins appear to play diverse roles as components of various protein complexes to orchestrate transcriptional programs in multiple tissues.

Although acquired *Pbx1* somatic mutations are associated with hematopoietic cancer (Hunger, 1996), the lack of *Pbx1* germline mutants has compromised a refined analysis of its in vivo contributions to mammalian development. In this report we have generated and characterized *Pbx1*-deficient mice. *Pbx1* is an essential gene, whose loss results in late gestational lethality, accompanied by severe hypoplasia or aplasia of multiple organs. A necessary role in patterning is apparent from widespread defects of the axial and appendicular skeleton, including morphological transformation of skeletal elements of the second branchial arch. Furthermore, absence of Pbx1 causes abnormalities in chondrocyte proliferation and differentiation, which result in precocious ossification and bone formation. These studies reveal a novel function of *Pbx1* in coordinating the extent of chondrocyte proliferation and terminal differentiation, suggesting a mechanistic basis for most of the observed skeletal malformations.

MATERIALS AND METHODS

Targeted disruption of the *Pbx1* gene and generation of *Pbx1* knockout mice

The *Pbx1* gene was mutated by insertion of a PGK-neo cassette (from the pNT vector) into the unique *Nhe*I site of exon 3, the largest 5′ exon containing a non-unit number of codons. An 8.5 kb segment of genomic DNA spanning the disrupted *Pbx1* exon 3 was then cloned into the targeting vector containing the Herpes Simplex Virus thymidine kinase (HSV-tk) cassette (Fig. 1). The targeting construct was linearized by *Not*I digestion and then electroporated into ES cells (TL1 line; Labosky et al., 1997). Following positive/negative selection in G418 and gancyclovir, homologous recombinant clones were identified by Southern blot analysis using three different enzyme and probe combinations (5′ and 3′ external probes and a neo-specific internal probe). Out of 95 informative clones, 8 yielded restriction digest patterns diagnostic for homologous recombination. Euploid clones were micro-injected into C57BL/6J host blastocysts. Chimeric male mice from two independently derived ES clones (38 and 176) passed the targeted *Pbx1* allele through the germline. Phenotypes were analyzed in embryos derived from the third backcross generation on a C57BL/6 background and on a fully inbred 129/SvTer background. The homozygous (−/−) phenotype was identical in mice derived from either of two independently targeted ES clones (38 and 176). Genotype analysis was performed on DNA extracted from tail biopsies of adult mice or from yolk sacs of embryonal conceptuses (E10-19) dissected free of maternal tissues. Following digestion with *Ssp*I, DNAs were subjected to Southern blot analysis using the *Pbx1* 3′ external probe.

Western blot analysis

Whole embryos at E16 were lysed in 2× SDS sample buffer following homogenization using established procedures (Jacobs et al., 1999). Proteins were subjected to SDS-polyacrylamide gel electrophoresis and immobilized on nitrocellulose filters following electrophoretic transfer. Pbx1 proteins were detected by western blot analysis using a monoclonal antibody (αPbx1b) specific for the Pbx1b isoform (the most abundant of two translation products that arise from differential splicing of the Pbx1 transcript) or an anti-Pbx1 rabbit antiserum raised against the amino terminus of Pbx1 (P-20; Santa Cruz Biotechnology).

Histology and immunohistochemistry

For histological analysis, embryos were fixed in formalin and embedded in paraffin for sectioning using standard procedures. Sections of 5 μm thickness were stained with Hematoxylin and Eosin (H and E) and von Kossa, mounted in DPX and photographed. Immunohistochemistry was performed on dewaxed, paraffin sections following microwave antigen retrieval (when necessary for select antibodies). Primary antibodies consisted of: Pbx1b-specific (αPbx1b) and pan Meis-specific monoclonal antibodies (Ab) (Jacobs et al., 1999); polyclonal anti-collagen X (Kwan et al., 1997) (generously provided by Olena Jacenko); monoclonal anti-PCNA and polyclonal antisera against collagen II, MMP-2, MMP-3 and MMP-9 (all purchased from Santa Cruz Biotechnology); monoclonal anti-BrdU (purchased from Neo Markers).

Analysis of BrdU incorporation

Pregnant mice were injected intravenously with 50 μg bromodeoxyuridine (BrdU) per gram of body weight 3 hours before sacrifice. Embryos were treated as above and embedded in paraffin before transverse sectioning. BrdU was detected by immunohistochemistry as described previously (Nowakowski et al., 1989) and sections were counterstained lightly with H and E. All BrdU-positive (dark brown) and -negative (blue) nuclei were counted over various rib sections. At least 15 different sections were counted for each of two wild-type and two *Pbx1*$^{-/-}$ littermate embryos at E12.5, 13.5 and 14.5.

Skeletal preparations

Differential staining of cartilage and bone in whole mouse embryos (E16) was visualized using Alcian Blue and Alizarin Red S (Mcleod 1980; Depew et al., 1999).

Whole-mount in situ hybridizations

Whole-mount in situ hybridizations were performed on embryos at E9.5, E10.5 and E11.5 as previously described (Wilkinson and Green, 1990). Hybridization probes for the clustered Hox genes (*a3*, *b1*, *b9*, *d3*, *d9* and *d11*) and branchial arch markers (*Lhx6*, *dHAND*, *Gsc*, *Hoxa2*) have been described in previous studies and their compositions are available upon request. All probes were labeled with digoxigenin, using standard procedures.

Section in situ hybridizations

In situ hybridizations were performed both on paraffin and frozen sections, of embryos at E12.5, E13.5 and E15.5, using digoxigenin and ^{35}S-labeled riboprobes, as previously described (Wilkinson, 1992). Single stranded sense and antisense riboprobes were generated which were specific for Indian hedgehog (*Ihh*; Bitgood and McMahon, 1995), *Sox9* (Wright et al., 1995; Ng et al., 1997), *Fgfr3* (Deng et al., 1996), parathyroid hormone-related peptide and its receptor, *PTHrP* and *PTHrPR* (Lanske et al., 1996), *Col2a1* type IIA form, *Col10a1* and *Col1a1* (Cheah et al., 1995). In situ hybridizations were carried out on adjacent sections to facilitate comparison of the expression patterns.

RESULTS

Pbx1 is essential for fetal development

A null allele of the endogenous mouse *Pbx1* gene was created by insertion of a neomycin resistance gene into exon 3 through homologous recombination in ES cells (Fig. 1). The

Fig. 1. Targeted inactivation of *Pbx1* and gross morphology of wild-type and mutant embryos. (A) Schematic representation of the mouse *Pbx1* cDNA, genomic locus, targeting vector and mutated allele following homologous recombination. In the *Pbx1* cDNA, sequences derived from exon 3 and the homeodomain (HD) are shown as black and gray boxes, respectively. Approximately 20 kb of the *Pbx1* locus flanking exon 3 (black box) are depicted along with mapped restriction sites. The targeting construct carries a *PGK-neo* cassette, inserted into the unique *Nhe*I site of *Pbx1* exon 3, and the *HSV-tk* gene, shown as solid white boxes. The transcriptional orientations of the *Pbx1* arms of homology are opposite to that of the *PGK-neo* cassette. The 5′ and 3′ external probes used for Southern blot analyses are shown as solid black boxes below the mutated allele. Restriction enzyme sites: E, *Eco*RI; N, *Nhe*I; S, *Ssp*I; X, *Xho*I. *Xma*I and *Not*I sites are in the targeting vector; the *Ssp*I site (**S**) was introduced to facilitate diagnostic analysis. (B,C) Southern blot analysis of *Pbx1* alleles. DNA from cell lines (B) or mouse tissues (C) was analyzed with probes and enzymes indicated beneath the panels. Wild-type (16 and 6.5 kb) and mutant (7.2 and 5.5 kb) *Pbx1* alleles for *Xma*I and *Ssp*I digests, respectively, are indicated to the right of each panel. TL, ES cell line used for *Pbx1* gene targeting; clones 38 and 176, targeted ES cells that passed the *Pbx1* mutation through the germ line; MEFs, mouse embryonic fibroblasts. (D) Western blot analysis of Pbx1b expression. Protein extracts of E16 embryos were subjected to western blot analysis using a monoclonal antibody specific for the Pbx1b isoform. Genotypes determined by Southern blotting are listed at the top. Right lane contains in vitro translated Pbx1b. Migrations and sizes (kDa) of molecular mass standards are indicated to the right. (E,F) Gross morphology of wild-type and *Pbx1*−/− embryos at E13.5 (E) and E16 (F). Mutant embryos display massive subcutaneous edema (yellow arrowhead), pallor, slender thorax and abdomen, hypoplastic pinna (red arrowhead) and atypical hunched posture with abnormal orientation of both hind- and forelimbs (black arrowheads).
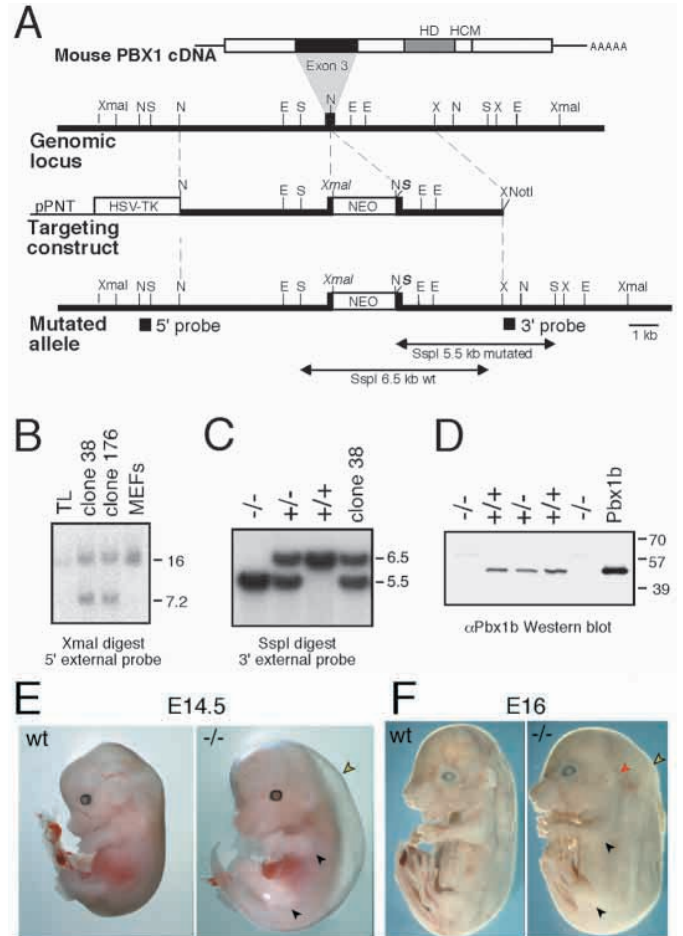
expected wild-type and mutated *Pbx1* alleles were observed by Southern blot analysis of DNA extracted from targeted ES cell lines and mouse tissues (Fig. 1B,C). Western blot analysis of embryos at E16 showed that homozygous mutant embryos expressed neither full-length Pbx1b proteins (Fig. 1D) nor truncated amino-terminal fragments of Pbx1 (data not shown).

Pbx1+/− mice expressed half the normal level of Pbx1b proteins (Fig. 1D) but were viable, fertile and displayed no apparent abnormalities other than a decreased size (30% by weight prior to 8 weeks of age). Intercross matings of *Pbx1*+/− mice yielded no viable *Pbx1*−/− pups with the exception of one stillborn neonate out of 77 F2 offspring (Table 1). Binomial proportion analysis showed no deviations from a 2:1 heterozygote:wild-type ratio (Table 1), suggesting that *Pbx1* null embryos died during gestation.

Pbx1−/− embryos from timed intercross matings were analyzed to determine the specific stage of embryonic lethality (Table 1) and to study the lethal phenotype. Prior to E12.5, *Pbx1*−/− embryos could not be distinguished morphologically from wild-type or heterozygous embryos. Subsequently, mutant embryos showed massive and progressive subcutaneous edema (Fig. 1E). They also exhibited generalized pallor, diminished vascularization, slender thorax and abdomen, hunched posture, abnormal orientation of both the fore and hind limbs, and hypoplastic ear pinnae (Fig. 1E,F). Furthermore, in *Pbx1*−/− embryos many internal organs were severely hypoplastic (e.g. lungs, liver, stomach, gut, kidneys

and pancreas), ectopic (thymus, kidneys) or aplastic (spleen) (Table 2 and data not shown). Nonetheless, until E14.5 all *Pbx1*−/− embryos were alive, as evidenced by heart beat and pulsation of arterial blood through the umbilical artery, and were obtained in the expected Mendelian ratio (Table 1). Thereafter, an increasing number of *Pbx1*−/− embryos were dead, beginning at E15.5, and none were alive at E17.5 (Table 1). These data established that *Pbx1* is an essential gene whose loss results in late gestational lethality. Here we focus on the phenotypic consequences of the loss of Pbx1 in the developing skeleton.

Table 1. Genotypes of embryos obtained from intercrosses of *Pbx1*+/− mice

Stage	Total	+/+	+/−	−/− Alive	−/− Dead	Necrotic*
E11.5	37	12	15	10	0	0
E12.5	29	8	14	7	0	0
E13.5	33	9	14	10	0	0
E14.5	56	8	39	9	0	0
E15.5	50	11	22	12	5	0
E16.5	30	7	15	4	4	0
E17.5	28	6	11	0	5	6
E18.5	29	5	15	0	4	5
F2 Pups	77	26	50	0	1	0

*Genotyping was not possible.

Fig. 2. Pbx1 expression and skeletal structures in wild-type and mutant embryos.
(A-D) Immunohistochemical analysis of Pbx1b localization visualized with DAB (brown staining) on tissues counter-stained with Hematoxylin. Diffuse nuclear Pbx1b expression is present in the epidermis and mesenchymal tissues of the embryo at E13.5 (A), most intensely in mesenchyme that is condensing to form rib (black arrowheads) and vertebral (red arrowheads) cartilage (B). Abundant Pbx1b expression in proliferating rib chondrocytes at E14.5 (C), which is nuclear (C, inset), is reduced to undetectable levels in hypertrophic chondrocytes at E16 when ossification is imminent (D). BA2, second branchial arch; vert, vertebrae. (E,F) Differential bone and cartilage staining of skeletal elements. E16 embryos were stained with Alcian Blue and Alizarin Red to visualize cartilage and bone, respectively, in the forming skeletal structures. Lateral views demonstrate agenesis of the ventral ribs, hypoplasia of the sternum and clavicles, together with rib malformations and fusions (red arrowhead) in the *Pbx1*^{−/−} embryo (E, right). There is also thinning, compressions (black arrows) and fusions (red-tipped arrows) of the vertebral bodies and neural arches in the *Pbx1*^{−/−} embryo (F, bottom). The

styloid process and hyoid lesser horns (green arrows) are malformed, as are the structures of the occipital arch. Costal cartilage, Cc; clavicle, cv; exoccipital, EO; otic capsule, OC; ossified rib, orb; supraoccipital arch, SOA; sternum, stn. Asterisks indicate malformed structures.
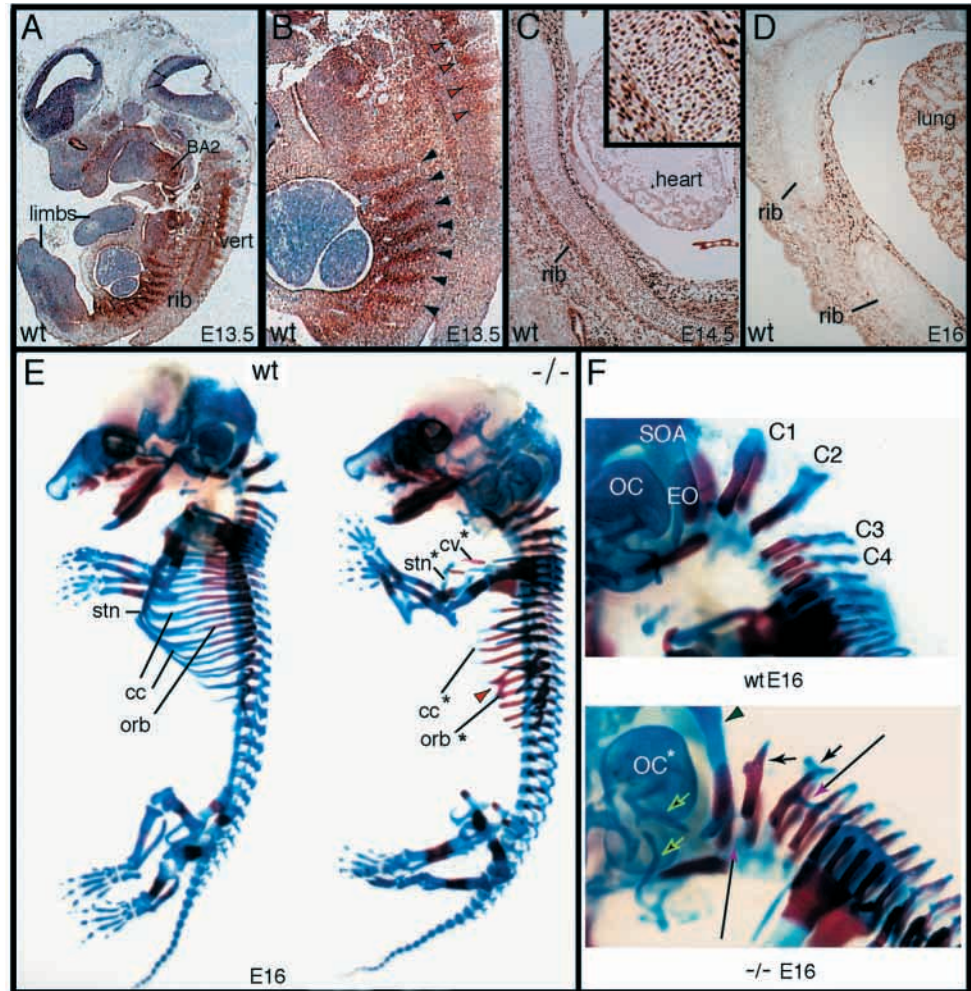
Pbx1^{−/−} embryos display axial skeletal malformations that are not segmentally restricted

Previous studies have shown that *Pbx1* is transcribed widely throughout the embryo (Roberts et al., 1995; Schnabel et al., 2001). Nuclear-localized Pbx1 protein was detected by immunohistochemistry in many immature epithelial and mesenchymal cells, particularly in condensing pre-cartilagenous mesenchyme (Fig. 2A,B). It was also highly expressed in the nuclei of proliferating chondrocytes at E14.5 (Fig. 2C), but progressively decreased with further chondrocyte maturation and was undetectable in hypertrophic chondrocytes at the onset of ossification (Fig. 2D). Consistent with this expression profile, *Pbx1*^{−/−} embryos showed widespread abnormalities involving both the axial and the appendicular skeleton (Fig. 2E).

Within the axial skeleton, agenesis of the ventral portions of all 13 ribs was observed, together with thickening and fusions (arrowhead) of shortened ribs (Fig. 2E). The sternum was severely hypoplastic (Fig. 2E). The cervical and thoracic vertebrae were thinned, their arches were occasionally fused (black arrows), and the intervertebral spaces were reduced (Fig. 2E,F). These features were most severe in the C1, C2 and

C3 cervical vertebrae. The expected numbers of vertebrae were observed and the vertebral and rib malformations showed some left-right asymmetries (data not shown). In addition to the vertebral alterations, the cranial skeletal elements derived from the occipital arch (exoccipital and supraoccipital), otic capsule and parachordal plate (basioccipital and basisphenoid) were abnormal (arrowhead Figs 2F, 3C). Thus, *Pbx1*^{−/−} mice displayed widespread axial skeletal malformations.

Anterior homeotic transformation of second branchial arch structures in *Pbx1*^{−/−} embryos

Structures derived from the second branchial arch and first pharyngeal groove displayed striking morphological changes in *Pbx1*^{−/−} mutants. The main source of ectomesenchyme in the second branchial arch, the rostral-most Hox-positive arch, is cranial crest-derived from rhombomere 4 (Couly et al., 1996; Kontges et al., 1996). Nuclear Pbx1 was detectable by immunohistochemistry in the ectomesenchyme and ectoderm of the second branchial arch and around the first pharyngeal groove at E11.5, while the ectomesenchyme of the mandibular and maxillary branches of the first branchial arch showed much lower nuclear immunoreactivity (Fig. 3A). Consistent with the

Fig. 3. Transformation of second branchial arch cartilages into structures resembling mandibular first arch cartilages in *Pbx1*$^{-/-}$ embryos as determined from anatomic, histological and molecular analyses.

(A) Immunohistochemical analysis shows extensive Pbx1b expression in mesenchyme of the second branchial arch and first pharyngeal groove of E11 and E13.5 wild-type embryos (transverse section). Auricular pinna, AP; first branchial arch, BA1; second branchial arch, BA2; Meckel's cartilage, MC; mandibular arch, MdA; maxillary arch, MxA; optic cup, opc; otic capsule, OC; first pharyngeal groove, PG1; styloid process, SP; spinal cord, spc; tongue, Tg.

(B) Lateral views of wild-type (top) and mutant (bottom) E16 head skeleton. The lesser horns of the mutant are greatly elongated, resembling Meckel's cartilage (or BA2 homologs of non-mammalian vertebrates). They extend from the hyoid body and end adjacent to the styloid process. The stapes is absent, and the styloid process is also dysmorphic, being shorter, thicker and having an ectopic flange (yellow arrowhead). Its shape resembles, in parts, a malleus. Proximocaudal madibular arch structures are slightly dysmorphic, as exemplified by the caudal border of the malleus. There is a small, ectopic cartilaginous spicule near the malleus (green arrowhead).

(C) Inferior views of the wild-type (left) and mutant (right) head showing the branchial arch defects, in addition to malformations (red arrowhead) of the cranial base. Green and yellow arrowheads denote structures described in B.

(D) Morphologies of dissected hyoid and mandible cartilages. Asterisks indicate malformed structures. Abbreviations: atlas, at; dentary, dnt; exoccipital, eo; greater horn of hyoid, gh; hyoid body, hb; incus, in; lesser horn of hyoid, lh; transformed lesser horn of hyoid bone, lh*; malleus, ma; Meckel's cartilage, MC; nasal capsule, nc; otic capsule, OC; supra capsular fissura, scf; styloid process, sp.

(E) Histology of H and E-stained

transverse sections of wild-type and *Pbx1*$^{-/-}$ embryos at E16. The transformed and elongated lesser horns of the hyoid bone are indicated by an asterisk. greater horn of hyoid, gh; lesser horn of hyoid, lh; transformed lesser horn of hyoid bone, lh*; Meckel's cartilage, MC; oropharynx, o. (F) Same as E, magnified 100×. The transformed lesser horn of the hyoid consists of tightly packed, proliferating chondrocytes. (G,H) Whole-mount in situ hybridization analysis of *Lhx6* and *dHAND* expression in wild-type and *Pbx1*$^{-/-}$ embryos at E10.5.
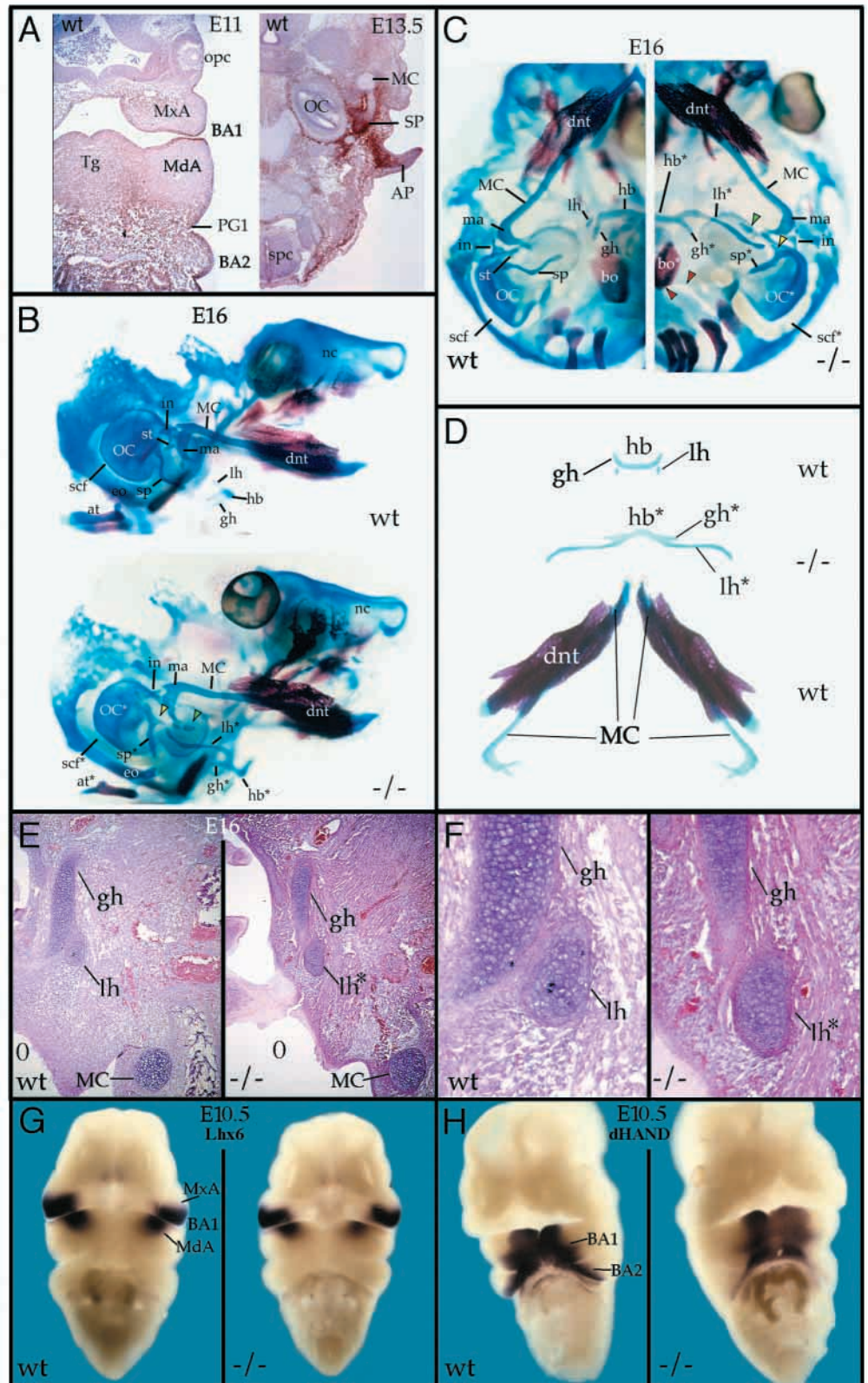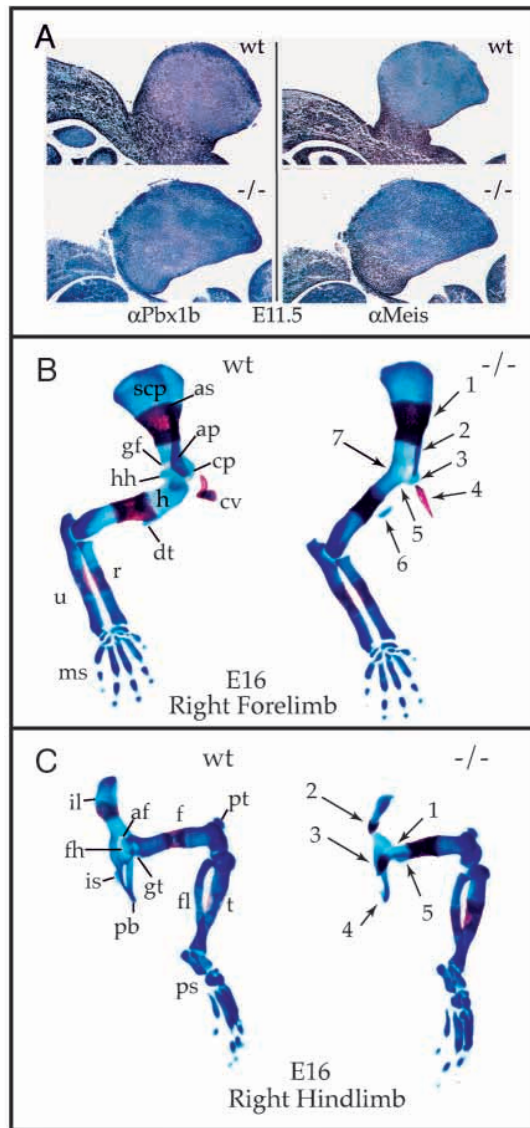
Fig. 4. Malformations of proximal but not distal appendicular skeletal structures in *Pbx1⁻/⁻* embryos. (A) Immunohistochemical analysis using anti-Pbx1b (αPbx1b) or anti-Meis (αMeis) antibodies on transverse sections of limb buds from E11.5 wild-type and *Pbx1⁻/⁻* embryos. Diffuse nuclear expression (brown) of Pbx1b and Meis is detected in superimposable domains confined to the proximal limb buds of wild-type embryos. In limb buds of *Pbx1⁻/⁻* embryos, both nuclear and cytoplasmic expression of Pbx1b is absent, while Meis protein expression is unperturbed. (B) Skeletal structures in right forelimb of wild-type (left) and *Pbx1⁻/⁻* (right) E16 embryos. The morphologies of the limbs with associated scapulae and clavicles dissected free from embryos are shown in lateral views. In the *Pbx1⁻/⁻* embryo, there is hypoplasia of the superior scapular border (1), acromial spine and process (2), and coracoid process (3). The clavicle is shortened and attenuated (4). The humerus is shorter, distorted and thinned proximally; its head is fused to the glenoid cavity (5) and coracoid process (3) and continuous with the inferior border of the scapula (7). The cartilaginous core of the deltoid tuberosity is nonconjoined (6). The cartilages of the distal forelimb are spared. acromial process, ap; acromial spine, as; coracoid process, cp; clavicle, cv; deltoid tuberosity, dt; glenoid process, gf; humerus, h; humeral head, hh; manus, ms; radius, r; scapula, scp; ulna, u. (C) Lateral views show the morphology of the pelvic girdle, with malformed and rudimentary ilium (2), ischium (3) and pubis (4), in the *Pbx1⁻/⁻* hindlimb (right). The os coxae-femur articulation (1) is fused. The hindlimb malformation also affects the femur, which is shorter and distorted proximally (5) in the *Pbx1⁻/⁻* embryo, while the cartilaginous structures of the distal hindlimb are spared. acetabular fossa, af; femoral head, fh; femur, f; fibula, fl; greater trocanter, gt; ilium, il; pubis, pb; pes, ps; patella, pt; tibia, t.

splanchnocranial cartilage derived from this tissue. The lesser horn of the hyoid was morphologically transformed into an elongated cartilage whose structure was reminiscent of Meckel's cartilage (a derivative of the mandibular branch of the first branchial arch) or of the suspensorial second arch derivatives of certain non-mammalian vertebrates (Fig. 3B-D). This cartilage extended from the body of the hyoid, with which it was fused, to an ectopic flange on the styloid process. The styloid process itself was thickened and truncated; its structure also displayed characteristics of the malleus, a first arch-derived cartilage. The mutants lacked stapes and oval windows in the otic capsules (Fig. 3B,C). A small ectopic cartilaginous structure formed adjacent to the malleus (green arrowhead Fig.

strong nuclear expression in the second branchial arch, *Pbx1⁻/⁻* mutants had a striking morphological alteration in the

Table 2. Phenotypic overlaps in *Pbx1* and *Hox* knockout mice

Pbx1 phenotype	Hox* null mutants	Hox Reference
Anterior transformation of BA2	*Hoxa2*	Rijli et al., 1993; Gendron-Maguire et al., 1993
Cervical vertebral malformations	*Hoxa3/b3/d3*	Manley and Capecchi, 1997
Rib malformations	*Hoxa9/b9*	Chen and Capecchi, 1997
Forelimb skeletal malformations	*Hoxa9/d9*	Fromental-Ramain et al., 1996
Proximal hindlimb skeletal malformations	*Hoxa10*	Favier et al., 1996
Cranial nerve defects‡	*Hoxa1/b1*	Gavalas et al., 1998
Impaired hematopoiesis§	*Hoxa9/c8*	Lawrence et al., 1997; Shimamoto et al., 1999
Ectopic thymus¶	*Hox3 paralogs*	Manley and Capecchi, 1998
Spleen agenesis**	*Hox11‡‡*	Roberts et al., 1994; Dear et al., 1995
Pancreas abnormal development and function§§	*Pdx1‡‡*	Jonsson et al., 1994; Offield et al., 1996

*All listed clustered and non-clustered Hox proteins bear Pbx1 dimerization motifs.
‡Depew and Selleri, unpublished observations.
§DiMartino et al., 2001.
¶Manley, Selleri and Cleary, unpublished.
**Selleri et al., unpublished.
‡‡Non-clustered *Hox* genes.
§§Kim et al., unpublished.

Fig. 5. Accelerated chondrocyte maturation in malformed skeletal structures of *Pbx1⁻/⁻* embryos. Histologic analysis shows H and E and von Kossa-stained transverse sections of wild-type and *Pbx1⁻/⁻* embryos. Aggregations of small chondrocytes are present in the ribs of wild-type (A,B) and *Pbx1⁻/⁻* (C,D) embryos at E13.5. In *Pbx1⁻/⁻* embryos, the center of the growing rib cartilage (green arrows) shows subtle morphologic features of more advanced chondrocyte maturation evidenced by the presence of more cells with small nuclei and large lipid droplets (black arrowheads). At E15.5, the *Pbx1⁻/⁻* rib (G,H) is prematurely comprised exclusively of hypertrophic chondrocytes, some clearly undergoing autolysis (red arrowhead, inset in H), and surrounded by extensive perichondral bone formation (blue arrows). In contrast, normal chondrocyte maturation appears to be present in the distal forelimbs of wild-type (I, J) and *Pbx1⁻/⁻* (K, L) embryos. At E 15.5, von Kossa staining shows the presence of extensive calcium deposits in *Pbx1⁻/⁻* rib cartilage (N), that are practically absent from wild-type cartilage (M). Magnifications: A,C,E,G,I,K (20×); B,D,F,H,J,L (40×); M, N and insets in F,H (100×).
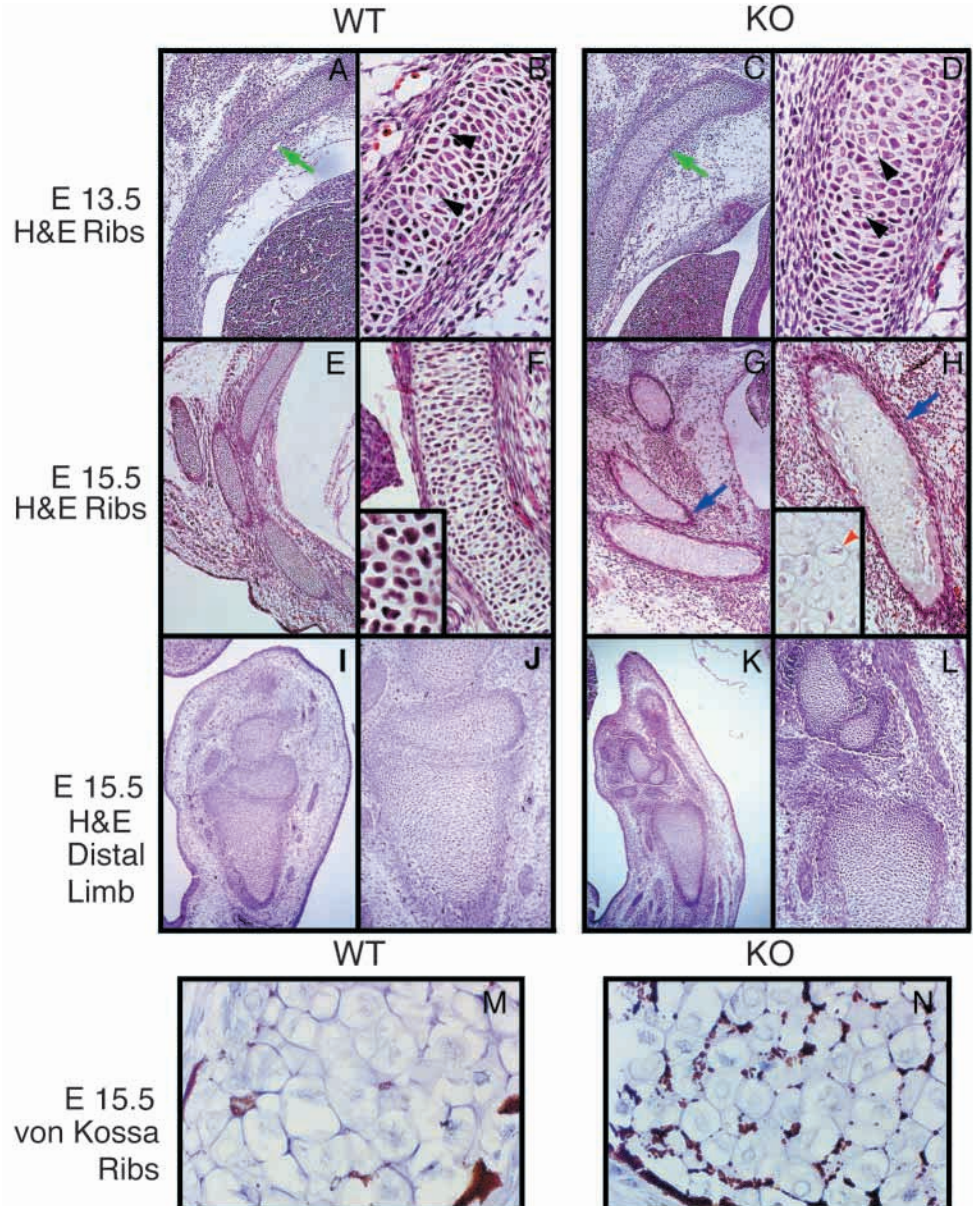
3B,C). The malleus was slightly dysmorphic at its articulation with the incus and along its caudal border. The pinnae of the ears, which develop around the first pharyngeal groove, were hypoplastic and malformed (Fig. 1F). Therefore, loss of *Pbx1* transformed second branchial arch cartilages into structures resembling splanchnocranial elements of the first branchial arch. Histologic analysis of BA2 at E16 (Fig. 3E,F) further showed an elongated structure, reminiscent of Meckel's cartilage, consisting of small proliferating tightly packed chondrocytes, in place of the lesser horns of the hyoid.

Several molecular markers of branchial arch development were examined at E10.5 to determine their roles in transformation of branchial arch morphology associated with the loss of *Pbx1*. These consisted of genes normally expressed exclusively in BA1 (*Lhx6*), genes normally expressed in the mesenchyme of BA2 (*Hoxa2*), and genes with proximodistally restricted expression within the branchial arches (*dHAND*, *Gsc*). We detected no major changes in the expression of these genes (Fig. 3G,H and data not shown).

Malformations of the proximal but not distal appendicular skeleton in *Pbx1⁻/⁻* mutants

A possible role for Pbx1 in patterning the vertebrate limbs was suggested by its restricted nuclear localization within the proximal domains of the limb bud, a feature shared with its *Drosophila* homolog exd (González-Crespo et al., 1998). In E11.5 wild-type embryos, Pbx1 protein was strongly expressed in the nuclei of mesenchymal cells of the proximal limb bud, but not in those of the distal bud (Fig. 4A). Meis proteins were detected in mesenchymal cell nuclei in a similar proximally restricted pattern in both wild-type and *Pbx1⁻/⁻* embryos (Fig. 4A). These data are consistent with the regulation of Pbx1 nuclear import by Meis-related TALE proteins (Berthelsen et al., 1999) in developing proximal but not distal limb buds.

By E14.5, skeletal structures of the proximal limbs and limb girdles, tissues that normally express nuclear Pbx1, were clearly abnormal in *Pbx1⁻/⁻* embryos, and by E16 the scapula and clavicle were malformed and the humerus was fused to the scapula (Fig. 4B). The proximal humerus was hypoplastic and misshapen, and the deltoid tuberosity was not conjoined. In contrast, distal fore limb elements and joints of the zeugopod and autopod appeared normal (Fig. 4B). In the hind limbs, the

pelvic girdle and proximal femur were malformed with a rudimentary ilium, ischium and pubis, and the os coxae-femur articulation appeared to be fused (Fig. 4C). As with the fore limb, distal elements and joints of the hind limb appeared normal (Fig. 4C). Thus, limb development in mammals is likely compartmentalized into Pbx1-dependent (proximal) and Pbx1-independent (distal) domains, as in arthropods (González-Crespo et al., 1998).

Absence of Hox and Meis expression perturbations in *Pbx1*−/− embryos

No differences were observed between wild-type and *Pbx1*−/− embryos in the spatial and temporal expression profiles of several *Hox* genes that normally contribute to the specification of structures displaying malformations in the *Pbx1*−/− mice (data not shown). These analyses examined *Hoxa3* (cervical vertebrae, hyoid), *Hoxb1* (hindbrain), *Hoxb9* (sternum and ribs), *Hoxd3* (cervical vertebrae), *Hoxd9* (proximal fore limb), and *Hoxd11* (distal limbs), at two different days (E9.5 and E11.5) of gestation. Furthermore, no perturbations of Meis expression or subcellular distribution were observed in the proximal limb buds (Fig. 4A) and other structures (not shown) of *Pbx1*−/− embryos. Thus, Meis nuclear import was not dependent on the presence of Pbx1 protein.

Accelerated progression of endochondral ossification in *Pbx1*−/− embryos

Histologic analysis was conducted on the developing skeleton in domains that displayed gross morphologic differences between wild-type and *Pbx1*−/− embryos. At E13.5, wild-type hyaline cartilage of the ribs contained aggregations of small, tightly packed chondrocytes (Fig. 5A,B). Focally, in the central portions of the ribs, *Pbx1*−/− chondrocytes displayed subtle features of more advanced maturation compared to wild type, as shown by the presence of a significant number of cells with markedly vacuolated cytoplasms (Fig. 5C,D). At E15.5, marked differences in chondrocyte maturation were readily apparent (Fig. 5E-H). Many more hypertrophic chondrocytes were observed in affected *Pbx1*−/− cartilage compared to wild type. Numerous chondrocytes were clearly undergoing autolysis, surrounded by extensive bone formation beneath the perichondrium (Fig. 5G,H). Representative data are shown for whole embryos that were entirely sectioned and stained. In addition, von Kossa staining of E15.5 *Pbx1*−/− rib cartilages showed the presence of extensive calcium deposits that were practically absent from wild-type cartilage, even in areas where chondrocytes had undergone hypertrophy (Fig. 5M,N), which is indicative of precocious mineralization and
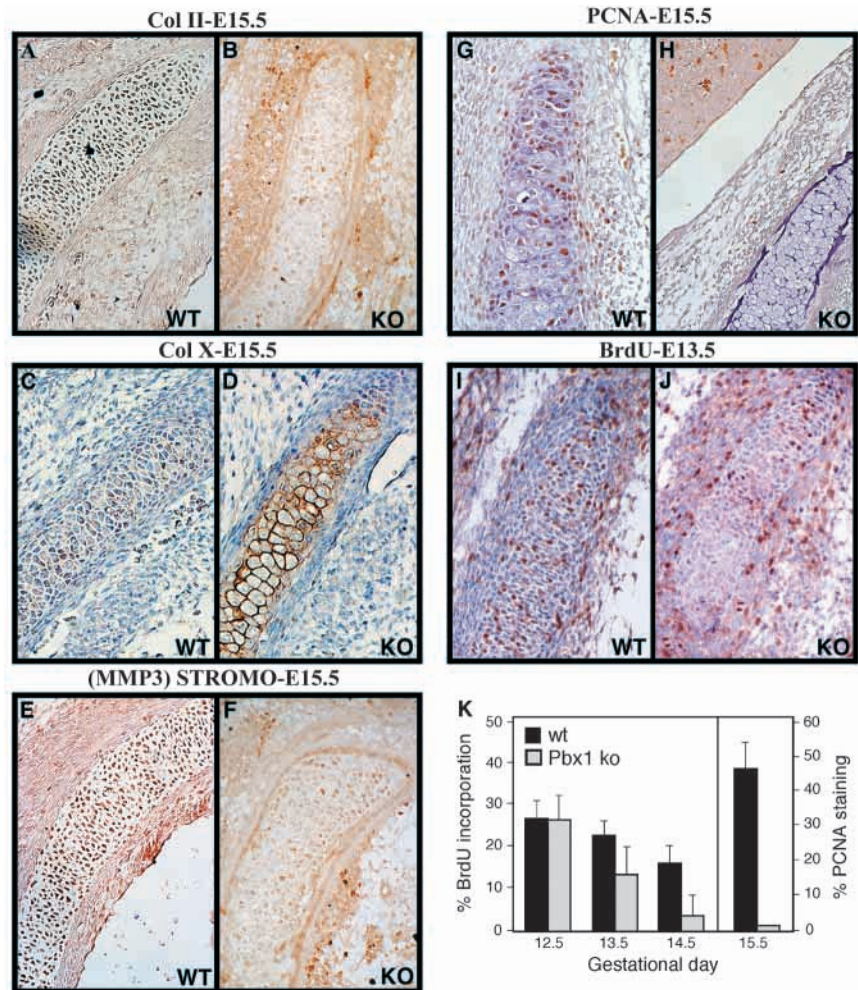
Fig. 6. Accelerated differentiation and diminished proliferation of chondrocytes in *Pbx1*−/− embryos, demonstrated by cell-type specific gene expression and cellular proliferation assays. (A-H) Immunohistochemistry was performed on serial sections of wild-type (left panels) and *Pbx1*−/− (right panels) cartilage at E15.5 using antibodies specific for markers of chondrocyte differentiation (A-F) and antibodies specific for cycling and dividing cells (G-J). Representative data are shown for embryos that were extensively sectioned and analyzed. (A,B) Collagen type II; (C,D) collagen type X; (E,F) stromolysin-1 (MMP3); (G,H) immunodetection of PCNA shows strong nuclear staining in numerous cells of wild-type but not *Pbx1*−/− rib cartilage at E15.5; (I,J) BrdU in vivo labelling shows a marked difference in the percentage of BrdU-positive nuclei (dark brown) between wild-type and *Pbx1*−/− rib cartilage at E13.5; (K) BrdU incorporation calculated as a percentage of BrdU-positive nuclei in rib cartilages at different developmental stages. Black bars, wild type; grey bars, *Pbx1*−/−. Percentage PCNA staining of wild-type (black) and *Pbx1*−/− (grey) at E15.5 is also shown. Bars represent means + s.d.

accelerated ossification of the mutant cartilage. Similar defects in chondrocyte differentiation were also seen in the proximal limbs (data not shown) but not in the distal limbs (Fig. 5I-L). Expansion of hypertrophic chondrocytes was not observed in the splanchocranium of BA2 (Fig. 3E).

Diminished chondrocyte proliferation in *Pbx1*−/− embryos

Growth within cartilagenous elements is dependent primarily on proliferation of chondrocytes prior to chondrocyte hypertrophy. Therefore, chondrocyte proliferation was

Fig. 7. Appropriate expression of chondrogenic regulators at early days of embryonic skeletogenesis and precocious bone formation in *Pbx1*$^{-/-}$ embryos. (A-R) In situ hybridizations were performed on sections of wild-type and *Pbx1*$^{-/-}$ rib cartilage at E13.5 and 15.5. (A-L) Digoxigenin-labeled riboprobes specific for candidate chondrogenic regulators were utilized on frozen sections. (A-D) *Ihh*; (E-H) *Sox9*; (I-L) *Fgfr3*. (D,H,L) Expression of these genes was physiologically lost in *Pbx1*$^{-/-}$ rib cartilage at E15.5, when many more hypertrophic chondrocytes are present, most of which are undergoing accelerated autolysis and precocious mineralization, compared to wild type (C,G,K). Rib cartilage boundaries in *Pbx1*$^{-/-}$ embryos at E15.5 are indicated by dotted lines in D,H and L. (M,P) Bright-field photos of serial sections consecutive/adjacent to those where in situ hybridization was performed (N-R). ^{35}S-labeled riboprobes for *Col1a1*, a marker of bone, and *Col10a1*, a marker of hypertrophic chondrocytes, were utilized on wax sections. In *Pbx1*$^{-/-}$ rib the presence of hypertrophic chondrocytes and scarce proliferating chondrocytes (P), is associated with advanced expression of *Col1a1* in the perichondrium of the rib (Q), indicative of the forming bone collar (green arrow). *Col10a1* expression is diminished in the middle of the mutant rib (R) presaging ossification and bone deposition. By contrast, in wild-type rib, proliferating chondrocytes (black arrow in M) are still present in large numbers and *Col1a1* is not expressed (N). However, *Col1a1* is expressed in the developing calvarial bones of both the wild-type and *Pbx1*$^{-/-}$ mutants (M and P: insets). *Col10a1* is expressed at high levels in wild-type rib (O). Representative data are shown for embryos that were extensively sectioned and analyzed.
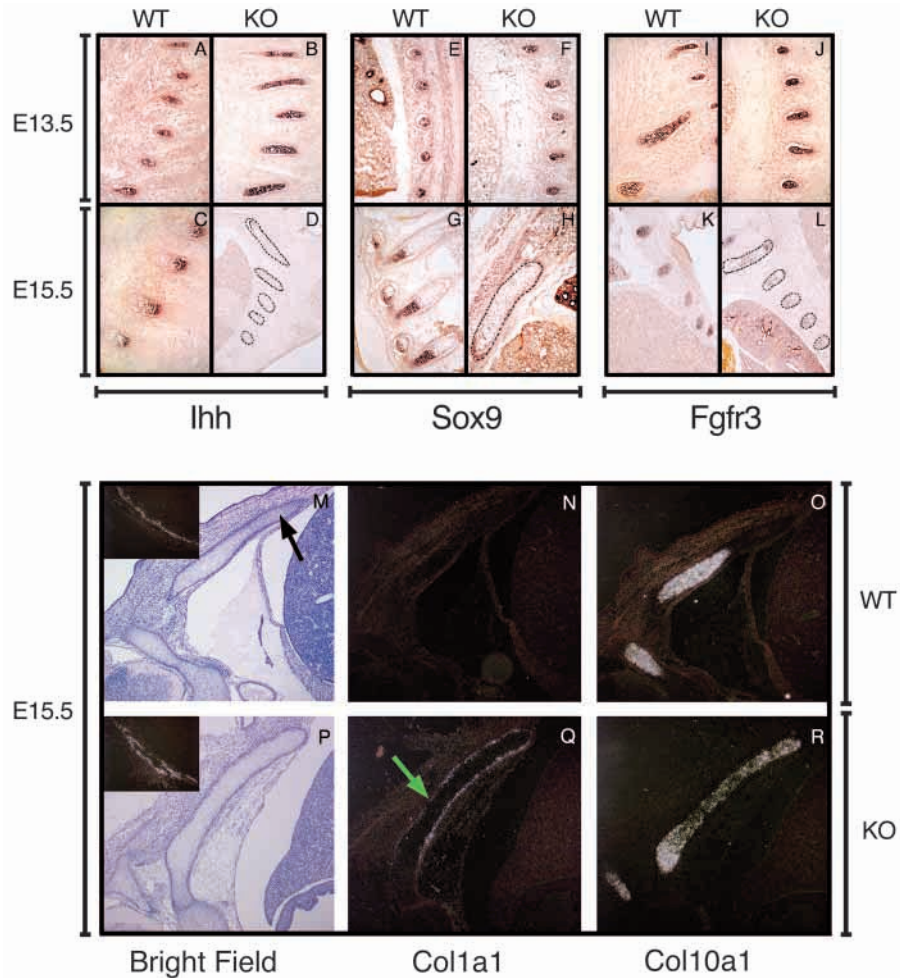

evaluated in *Pbx1*$^{-/-}$ mutants. Marked differences in the mitotic index of chondrocytes in wild-type and mutant rib cartilage were observed. At E15.5, numerous cells of wild-type rib cartilage (Fig. 6G) showed strong nuclear expression of PCNA (proliferating cell nuclear antigen; Hall et al., 1990), while in mutant rib cartilage no PCNA-positive cells were detected (Fig. 6H). BrdU (Nowakowski et al., 1989) in vivo labeling of embryos between E12.5 and E14.5 showed a striking reduction in the percentage of S-phase cells in *Pbx1*$^{-/-}$ rib cartilage compared to wild type (Fig. 6K). This difference was most marked at E14.5, but was also readily apparent at E13.5 (Fig. 6I,J). At E12.5, in contrast, no substantial differences in the percentage of BrdU-positive nuclei were detected in mesenchymal cells condensing to form *Pbx1*$^{-/-}$ rib cartilage compared to wild type (Fig. 6K). These observations demonstrate that the lack of *Pbx1* results in markedly diminished proliferation of chondrocytes between E12.5 and E13.5.

Precocious bone formation in *Pbx1*$^{-/-}$ mutants

To gain insight into molecular changes that may underlie the abnormal chondrocyte differentiation associated with the loss of *Pbx1*, the expression of genes characteristic for different stages of chondrocyte differentiation and maturation (Wai et al., 1998, Olsen et al., 2000) was examined for alterations in pattern and/or onset. Genes examined included the matrix genes *Col2a1* type IIA (Ng et al., 1993), *Col10a1* and *Col1a1* (Cheah et al., 1995) and genes that regulate chondrogenesis, such as *Fgfr3* and *Sox9* (Deng et al., 1996; Colvin et al., 1996; Ng et al., 1997; Bi et al., 1999), *Ihh* (St-Jacques et al., 1999), *PTHrP* and *PTHrPR* (Karaplis et al., 1994; Lanske et al., 1996).

Transcripts for *Col2a1* type IIA form (a marker of pre-chondrocytes and proliferating chondrocytes) were present in both wild-type and *Pbx1*$^{-/-}$ ribs at E12.5 and E13.5. Immunostaining showed that collagen II was expressed at E13.5 in both wild-type and *Pbx1*$^{-/-}$ ribs (data not shown). However, at E15.5, both *Col2a1* and collagen II were substantially reduced in *Pbx1*$^{-/-}$ rib cartilage, while expression was maintained in wild-type cartilage (Fig. 6A compared with B). At E13.5, staining for collagen X, which is characteristic of hypertrophic chondrocytes, was present in a few cells in wild-type ribs, but weak and more intracellular. By contrast, at E13.5, *Pbx1*$^{-/-}$ ribs showed distinct presence of collagen X in the matrix surrounding the hypertrophic chondrocytes (data not shown). This difference between *Pbx1*$^{-/-}$ and wild type was
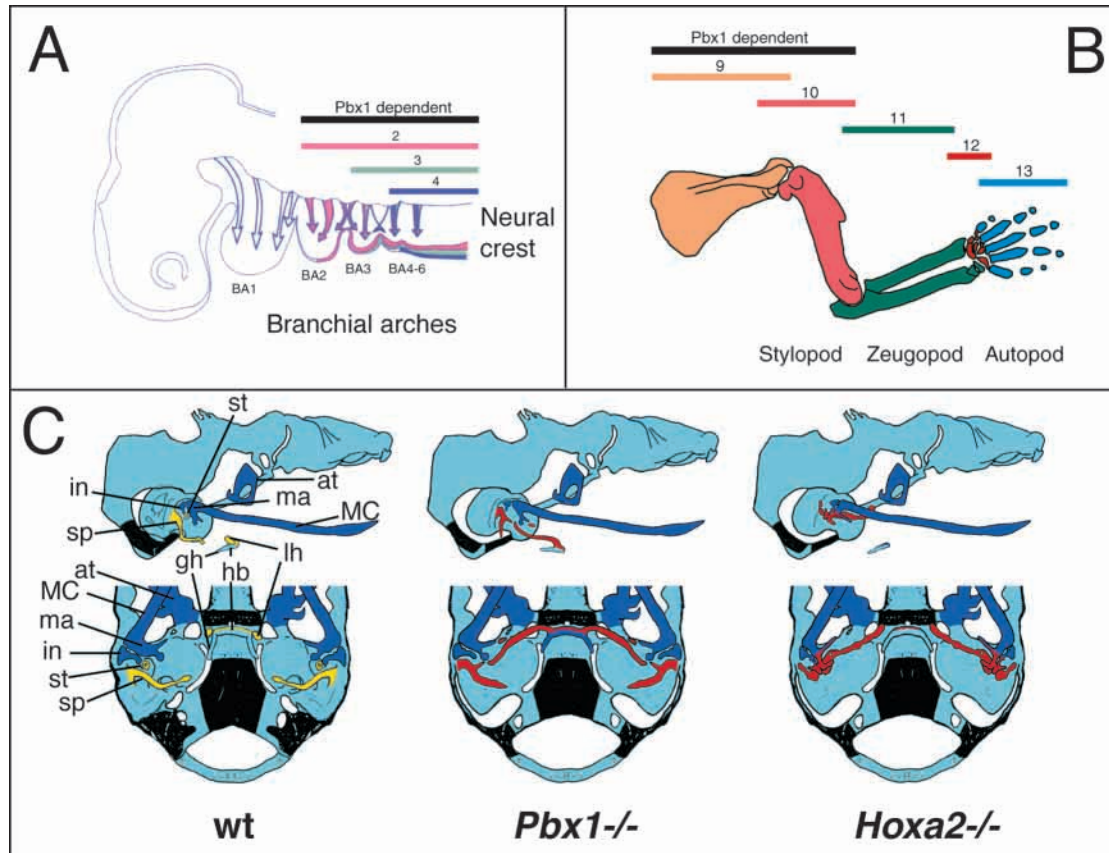
Fig. 8. Functional domains and relationships of the *Pbx1* and *Hox* genes in axial and appendicular skeletal morphogenesis. (A,B) Coloured lines indicate the anatomical regions affected by mutations in the *Pbx1* or *Hox* genes (paralog groups 9-13 in the limb and 2-4 in the ectomesenchymal component of the branchial arches). In the embryonic limb, Meis protein expression is spatially coincident with Pbx1-dependent regions and unperturbed in a *Pbx1* mutant background. B is adapted from Couly et al. (Couly et al., 1996). (C) Schemata depicting chondrocranial morphologies in wild-type, *Pbx1*$^{-/-}$ and *Hoxa2*$^{-/-}$ embryos at E16. The latter represents authors' interpretation of Rijli et al. (Rijli et al., 1992). Although not phenocopies, both *Pbx1*$^{-/-}$ and *Hoxa2*$^{-/-}$ mutants exhibit mandibular arch-like morphologies in the hyoid arch (BA2). Dark blue indicates BA1 structures, yellow, wild-type BA2 structures, and red, mutant BA2 structures at E16. Lateral views, upper panels; basal views, lower panels. ala temporalis, at; greater horn of hyoid, gh; hyoid body, hb; incus, in; lesser horn of hyoid, lh; malleus, ma; Meckel's cartilage, MC; styloid process, sp; stapes, st.

very prominent by E15.5 when collagen X was abundant in the extracellular matrix (and focal pericellular regions) of *Pbx1*$^{-/-}$ ribs (Fig. 6D), while staining was much less extensive in wild-type ribs that have only a few hypertrophic chondrocytes (Fig. 6C).

Rib cartilages were also evaluated for the presence of several matrix metalloproteinases normally expressed in chondrocytes (Ito et al., 1995; Nagase, 1998). At E13.5, MMP-2 (gelatinase A; Yu et al., 1998), MMP-9 (gelatinase B; Vu and Werb, 1998), and MMP-3 (stromelysin 1; Sternlicht et al., 1999) were present in both wild-type and *Pbx1*$^{-/-}$ cartilage. However, at E15.5 they were no longer detectable in *Pbx1*$^{-/-}$ cartilage (Fig. 6E,F and data not shown), providing further evidence that *Pbx1*$^{-/-}$ chondrocytes at E15.5 exhibited features of more mature cells.

No major changes in the overall patterns of expression of *Ffgr3* and *Sox9* (markers of proliferating chondrocytes), *Ihh* (marker of prehypertrophic chondrocytes), *PTHrP* and *PTHrPR* (markers of maturing and prehypertrophic chondrocytes) were detected in rib cartilages at early stages of skeletogenesis (E12.5 and 13.5; Fig. 7A-J and data not shown).

At E15.5 there were fewer cells positive for *Fgfr3, PTHrp* and *Sox9,* which is consistent with the strikingly reduced numbers of proliferating chondrocytes and the presence of many more hypertrophic chondrocytes that do not express these genes (Fig. 7G-L and data not shown). *Ihh* and *PTHrPR* were expressed appropriately in prehypertrophic chondrocytes in both wild-type and *Pbx1*$^{-/-}$ rib cartilage at the three stages examined. At E15.5, expression of these chondrogenic regulators was physiologically lost in *Pbx1*$^{-/-}$ hypertrophic chondrocytes of rib cartilage (Fig. 7C,D and data not shown), as expected, since most chondrocytes were undergoing accelerated autolysis and precocious mineralization (Fig. 5G,H,M,N).

In situ hybridization for *Col1a1*, a marker for bone, showed significant expression in the perichondrium surrounding the ribs in *Pbx1*$^{-/-}$ embryos at E15.5, while no signal was present in wild-type perichondrium, suggesting that bone formation was precocious (Fig. 7M-P). Taken together, these studies demonstrate that lack of *Pbx1* results in markedly diminished chondrocyte proliferation between E12.5 and E13.5 of mammalian endochondral skeletal development in non-cranial skeletal domains with grossly evident patterning defects. This

is associated with abnormal terminal differentiation (hypertrophy) and precocious bone formation by E15.5.

DISCUSSION

Mice lacking *Pbx1* function have abnormalities of several organs, many of which are either severely hypoplastic, ectopic, or aplastic (Table 2). Here we have focused on the consequences of *Pbx1* loss on skeletal development, including the morphogenesis of mesenchymal structures derived from the branchial arches and limb buds. These tissues can be segregated into *Pbx1*-dependent (caudal branchial arches and proximal limb buds) and *Pbx1*-independent domains (Fig. 8), demonstrating that *Pbx1* is part of an ancient code, some of whose features have been conserved from *Drosophila* exd to higher vertebrates, for establishment of the body plan. However, our studies also reveal a previously uncharacterized role for *Pbx1* in regulating the developmental programs of specialized cells in vertebrates, by temporally coordinating the extent of progenitor cell proliferation and commitment to terminal differentiation.

Essential role for Pbx1 in the refinement of multiple developmental programs

Pbx1$^{-/-}$ embryos die in utero and show diffuse patterning defects of the axial and proximal appendicular skeleton, as well as abnormalities in other organs. Some non-skeletal phenotypes, such as the spleen agenesis (Table 2), recapitulate phenotypes caused by the lack of 'orphan' Hox proteins, such as Hox 11, that bear Pbx dimerization motifs and heterodimerize with Pbx1 (Shen et al., 1996). The skeletal abnormalities, conversely, do not precisely recapitulate reported *Hox* null phenotypes (either single or compound; Capecchi, 1997) despite spatial overlap and morphological similarities. Their anatomic distributions, however, are associated with domains specified by Hox proteins containing tryptophan dimerization motifs essential for cooperative DNA binding with Pbx1 (Zákány and Duboule, 1999). Thus, the distal fore and hind limbs, which are specified by Hox proteins lacking Pbx dimerization motifs (paralogs 11-13), show no morphological abnormalities in *Pbx1*$^{-/-}$ embryos. This correlation, together with the various *Pbx1*$^{-/-}$ non-skeletal phenotypes overlapping Hox mutant phenotypes (Table 2), indicates that at least one role for Pbx1 in vivo is likely to be that of a selective Hox cofactor, whose actions are delimited by its capacity to dimerize with some, but not all, members of the Hox family. Consistent with this role, *Pbx1*$^{-/-}$ embryos show unperturbed spatial and temporal expression profiles of a representative subset of *Hox* genes that normally contribute to the specification of structures affected by the absence of *Pbx1*.

   In spite of the associations noted above, our observations that the skeletal malformations associated with loss of *Pbx1* do not precisely recapitulate individual *Hox* gene deficiencies raises the possibility of Hox-independent roles for Pbx1 in patterning. Indeed Pbx1 participates in diverse transcription complexes, only some of which are known to contain Hox components. However, overlapping expression of highly similar members of the respective Hox and Pbx protein families creates difficulty in unambiguously assigning specific

roles. Single or compound *Hox* null phenotypes represent not only loss of individual Hox function, but also the summation of relative overlapping contributions from other *Hox* genes that are co-expressed in the affected body segments (Krumlauf, 1994). Comparable *Hox* compensation, however, is unlikely to modulate the *Pbx1* phenotype if *Pbx1* globally compromises the actions of multiple Hox proteins that contribute to specification of individual body segments. It is also possible that loss of Pbx1 mimics a hypomorphic rather than null *Hox* phenotype, since not all Hox functions may be Pbx1 dependent. Finally, other members of the redundant Pbx family (Monica et al., 1991) may overlap with Pbx1 in their expression profiles and thus compensate for the loss of Pbx1 and ameliorate the nullizygous phenotypes.

   Loss of *Pbx1* is accompanied by a homeotic-like transformation in the second branchial arch (BA2) where, for example, the lesser horns of the hyoid are transformed into structures reminiscent of BA1-derived Meckel's cartilages. Similarly, in the zebrafish *Lazarus* mutant, BA2 cartilages, such as the hyosymplectic, are more similar to BA1 cartilages, such as the palatoquadrate (Popperl et al., 2000). We considered four possible mechanisms that may have contributed to the anterior-like transformation of BA2 to BA1-like morphology. These include loss of function of Hoxa2 protein in BA2, loss of expression of genes normally expressed in BA2 but not in BA1 (e.g. *Hoxa2*), gain of expression in BA2 of genes normally restricted to BA1 (e.g. *Lhx6*), and misexpression of genes normally proximodistally restricted within BA2 (*dHAND*, *Gsc*). Our data support the first scenario, since we observed no clear alterations in *Hoxa2*, *Lhx6*, *dHAND* and *Gsc* expression at E10.5. Like the *Pbx1*$^{-/-}$ mouse embryos, *Hoxa2* mouse mutants also display an anteriorization of the second arch skeleton (Fig. 7C), although there are differences in the nature of the morphologic transformation (Rijli et al., 1993). One explanation for the morphological differences between these mutants is that both genes have independent, as well as dependent functions in modifying the mandibular arch program to generate the hyoid arch program. Anterior transformation of second branchial arch-derived structures in *Pbx1*$^{-/-}$ embryos provides further support to the idea that the splanchnocranium of the first and second arches share common developmental programs (Rijli et al., 1993).

Pbx1 is obligatory for patterning the proximal-distal limb axis in vertebrates

Our results demonstrate that *Pbx1* is essential for patterning the proximal limbs in vertebrates, as its invertebrate homolog *exd* is required for patterning the proximal limbs of *Drosophila* (Gonzales-Crespo et al., 1998). In the fly limb, *exd* RNA and protein are broadly expressed, whereas nuclear localization of EXD protein is restricted to proximal regions (González-Crespo et al., 1998). In contrast, patterning of the distal fly leg, where EXD is cytoplasmic, is dependent on signaling by *wingless* and *decapentaplegic*, which are in turn activated by *hedgehog* (González-Crespo et al., 1998). In the mouse, the subcellular localization of Pbx1 in the developing limb parallels that of EXD in the *Drosophila* leg (González-Crespo et al., 1998; this study). This has led to the suggestion that the regulation of nuclear availability of Pbx/EXD cofactors controls the execution of Hox programs in limb development.

   Recent studies provide a molecular framework for the

control of proximal-distal limb specification and outgrowth based on antagonistic interactions conserved from insects to vertebrates. Ectopic expression of *Meis* genes in the distal limb of chicks induced proximalization of distal structures (Capdevila et al., 1999; Mercader et al., 1999). This suggested that normal restriction of Meis, and its invertebrate homolog homothorax (HTH), to the proximal regions of the vertebrate and insect limb, where Pbx1 is co-localized in the nucleus, is essential to specify cell fates and differentiation patterns along the proximal-distal axis. However, the complexity of Hox functions, their cross-regulation, and interactions with Meis/Pbx, make it difficult to conclusively interpret these ectopic expression data (reviewed in Vogt and Duboule, 1999). Conversely, the zebrafish *Lazarus* mutant dies very early, before vertebrae, posterior trunk and posterior fins develop (Popperl et al., 2000), making it impossible to assess the role of Pbx in proximal-distal limb specification in zebrafish. Our study unequivocally demonstrates that proximal-distal limb patterning in vertebrates, which is proposed to be controlled by Meis (Capdevila et al., 1999; Mercader et al., 1999), is dependent on the obligatory presence of Pbx1 in the proximal limb domain.

Requirement for Pbx1 in programming chondrocyte proliferation, terminal differentiation, and bone formation

Pbx1 mutants display defects in the development of specific endochondral skeletal elements. Endochondral bone development is a complex and tightly regulated process that requires programmed proliferation and maturation of chondrocytes followed by terminal differentiation, hypertrophy and replacement of cartilage by bone (reviewed by Karsenty, 1999; Olsen et al., 2000). Although $Pbx1^{-/-}$ cells appear to be capable of executing a complete program of endochondral ossification, as evidenced by the deposition of bone matrix in affected skeletal domains, the regulation of this process in affected elements is perturbed. Prior to E13.5, no clear histological differences were observed in the abilities of $Pbx1^{-/-}$ mesenchymal cells to condense and differentiate into proliferating chondrocytes. Similarly, at E13.5 histological analysis of both wild-type and $Pbx1^{-/-}$ embryos showed comparable collections of proliferating chondrocytes modeling the outlines of nascent skeletal elements. However, measurements of BrdU incorporation in vivo showed marked reduction in proliferation of $Pbx1^{-/-}$ chondrocytes at E13.5 and E14.5. By E15.5, the ribs of $Pbx1^{-/-}$ mutants completely lacked proliferating (PCNA$^+$) chondrocytes. Furthermore, histological and immunohistochemical studies show that chondrocytes of altered non-splanchnocranial elements had precociously matured to the terminal stage of chondrogenesis. Thus, lack of Pbx1 impacted the normal progression of chondrocyte terminal differentiation, resulting in disproportionate numbers of hypertrophic chondrocytes and precocious cartilage mineralization and bone formation. Whole embryo cartilage preparations also support this conclusion (data not shown). Performing whole embryo cartilage/bone staining at earlier days (E12.5-E14.5) could provide further support. Analogous perturbations in chondrocyte maturation may also have contributed to hyoid bone transformation, but in the form of enhanced, as opposed to attenuated, proliferation. The findings in $Pbx1^{-/-}$ mutant cartilage parallel our

observations that the hematopoietic defect in $Pbx1^{-/-}$ embryos results in part from deficiencies in the proliferative expansion of select hematopoietic progenitor cell populations (DiMartino et al., 2001). Thus, *Pbx1* may serve similar roles to orchestrate the growth and proliferation of progenitors at specific developmental stages within multiple cellular lineages.

Pbx1 does not have an upstream role in controlling the PTHrP-Ihh pathway that regulates chondrogenesis

The defective maturation and terminal differentiation of chondrocytes in *Pbx1* mutants could be the consequence of perturbations of the timing and/or extent of chondrocyte proliferation arising from altered expression of regulators of chondrogenesis. Many of the key regulatory molecules have been identified and insights into their roles gained from analyses of the impact of loss- or gain-of-function mutations on endochondral ossification in humans and mice (reviewed by Olsen et al., 2000). Such studies have shown that PTHrP and PTHrPR are important regulators of chondrocyte maturation acting to delay hypertrophy of chondrocytes. Loss of function in mice results in premature maturation of chondrocytes leading to excessive bone formation at birth (Karaplis et al., 1994; Vortkamp et al., 1996; Lanske et al., 1996). Although these phenotypes are similar histologically to those observed in the $Pbx1^{-/-}$ mutants, the endochondral bone development defect is widespread in PTHrP null mice (Karaplis et al., 1994), while it is restricted to specific skeletal segments in the absence of *Pbx1*.

Regulation of chondrogenesis by the PTHrP/PTHrPR pathway also involves other key regulators such as Sox9 and Ihh. The high-mobility-group domain transcription factor, Sox9, expressed throughout all cartilaginous condensations, is required for chondrogenesis (Bi et al., 1999). Recent studies suggest that Sox9 is a target of PTHrP signaling and that it may mediate some effects of PTHrP in the growth plate, inhibiting the maturation of pre-hypertrophic chondrocytes to hypertrophic chondrocytes (Huang et al., 2000). Ihh is a key signaling molecule, which stimulates chondrocyte proliferation and prevents chondrocyte hypertrophy through PTHrP-dependent and -independent pathways (St-Jacques et al., 1999; Vortkamp et al., 1996; Lanske et al., 1996). Lack of Ihh results in greatly reduced chondrocyte proliferation, delayed maturation, and poor bone formation. These changes in *Ihh* mutants are widespread in the skeleton, in contrast to the restricted distribution in *Pbx1* mutants (St-Jacques et al., 1999). Thus, *Ihh* and *Pbx1* mutants are very distinct from each other. *Fgfr3*-deficient mice also show defects in endochondral bone development. Unlike *Pbx1* mutants, they exhibit extended growth plates and striking overgrowth of the long bones (Colvin et al., 1996; Deng et al., 1996), thus revealing a function for Fgfr3 as a general negative regulator of chondrocyte proliferation. MMP-9 is also a key regulator of chondrogenesis but unlike Pbx1, the MMP-9 defect is restricted to the growth plate, and hypertrophic chondrocytes develop normally but ossification is delayed (Vu et al., 1998). Thus, despite some similarities, most features of the *Pbx1* mutant phenotype are distinct from those arising from loss of function of these known regulators of skeletogenesis. Furthermore, no major differences in the spatial or temporal expression of these chondrogenic regulators (*Ihh*, *PTHrP*,

PTHrPR, *Sox9* and *Fgfr3*) were detected in *Pbx1*⁻/⁻ rib cartilages.

Taken together, these results strongly suggest a model in which *Pbx1* is required to coordinate diverse facets of embryonic skeletogenesis via mechanisms that are likely distinct from known molecular pathways involving *PTHrP/PTHrPR/Ihh/Fgfr3*. The lack of major differences in expression of these regulators in *Pbx1* mutants indicates that Pbx1 is unlikely to be an upstream regulator of these genes at early stages of skeletal morphogenesis. Thus, a scenario could be envisaged where either Pbx1 functions downstream of these regulators of chondrogenesis, or alternatively Pbx1 may regulate chondrogenesis via collaborative interactions with other co-expressed factors that function in concert or in parallel, such as Sox9 or Hox proteins. Indeed, specificity of action by Sox9 is achieved via interactions with specific partner factors (reviewed by Kamachi et al., 2000). Moreover, combinatorial interactions among Pbx, Prep or Hox proteins have been shown to be involved in regulating tissue-specific production of collagen V (Penkov et al., 2000).

Given that we observed perturbations only in skeletal domains specified by Hox proteins bearing Pbx dimerization motifs, our results provide strong evidence that the requirement for Pbx1 in programming chondrocyte proliferation and maturation is Hox dependent. Indeed, a potential role of Hox proteins in the regulation of progenitor cell proliferation has been previously suggested based on studies of *Hox* null mice (Condie and Capecchi, 1993; Condie and Capecchi, 1994; Duboule, 1995). Furthermore, studies using retroviral vectors to misexpress *Hox* genes in chick limb bud (Goff and Tabin, 1997) have shown that *Hoxd11* and *Hoxd13* pattern the limb skeleton by regulating the rates of cell division in the proliferative zone of growing cartilage. Thus, a model in which *Hox* genes act as growth promoters has also been proposed (Goff and Tabin, 1997). Lastly, over-expression of a *Hoxc8* transgene has been shown to cause cartilage defects characterized by an accumulation of proliferating chondrocytes and reduced maturation (Yueh et al., 1998).

In summary, our studies reveal a previously unknown function for *Pbx1* as a component of the cellular machinery that determines the temporal coordination of progenitor cell proliferation and differentiation in vertebrates. Elucidation of the molecular basis for chondrogenic defects using intact animal models, such as the *Pbx1*-deficient mouse used here, will contribute to a better understanding of the different pathways that regulate skeletal development in vertebrates.

REFERENCES

Berthelsen, J., Zappavigna, V., Ferretti, E., Mavilio, F. and Blasi, F. (1998). The novel homeoprotein Prep1 modulates Pbx-Hox protein cooperativity. *EMBO J.* **17**, 1434-1445.

Berthelsen, J., Kilstrup-Nielsen, C., Blasi, F., Mavilio, F. and Zappavigna, V. (1999). The subcellular localization of PBX1 and EXD proteins depends on nuclear import and export signals and is modulated by association with PREP1 and HTH. *Genes Dev.* **13**, 946-953.

Bi, W., Deng, J.M., Zhang, Z., Behringer, R.R. and Crombrugghe, B. (1999). Sox9 is required for cartilage formation. *Nat. Genet.* **22**, 85-89.

Bischof L J., Kagawa, N., Moskow, J.J., Takahashi, Y., Iwamatsu, A., Buchberg, A. M. and Waterman, M.R. (1998). Members of the meis1 and pbx homeodomain protein families cooperatively bind a cAMP-responsive sequence (CRS1) from bovine CYP17. *J. Biol. Chem.* **273**, 7941-7948.

Bitgood, M. J. and McMahon, A. P. (1995). Hedgehog and Bmp genes are coexpressed at many diverse sites of cell-cell interaction in the mouse embryo. *Dev. Biol.* **172**, 126-138.

Burglin, T. R. (1997). Analysis of TALE superclass homeobox genes (MEIS, PBC, KNOX, Iroquois, TGIF) reveals a novel domain conserved between plants and animals. *Nucleic Acids Res.* **25**, 4173-4180.

Capdevila, J., Tsukui, T., Rodriguez Esteban, C., Zappavigna, V. and Izpisua Belmonte, J. C. (1999). Regulatory interactions between the proximal determinant Meis2 and distal antagonism of BMPs by gremlin control vertebrate limb outgrowth. *Mol. Cell* **4**, 839-849.

Capecchi, M. R. (1997). Hox genes and mammalian development. *Cold Spring Harbor Sym. Quant. Biol.* **62**, 273-281.

Chan, S. K., Jaffe, L., Capovilla, M., Botas, J. and Mann, R. S. (1994). The DNA binding specificity of Ultrabithorax is modulated by cooperative interactions with extradenticle, another homeoprotein. *Cell* **78**, 603-615.

Chang, C. P., Shen, W. F., Rozenfeld, S., Lawrence, H. J., Largman, C. and Cleary, M. L. (1995). Pbx proteins display hexapeptide-dependent cooperative DNA binding with a subset of Hox proteins. *Genes Dev.* **9**, 663-674.

Chang, C. P., Brocchieri, L., Shen, W. F., Largman, C. and Cleary, M. L. (1996). Pbx modulation of Hox homeodomain amino-terminal arms establishes different DNA-binding specificities across the Hox locus. *Mol. Cell. Biol.* **16**, 1734-1745.

Chang, C. P., Jacobs, Y., Nakamura, T., Jenkins, N. A., Copeland, N.G. and Cleary, M. L. (1997). Meis proteins are major in vivo DNA binding partners for wild type but not chimeric Pbx proteins. *Mol. Cell. Biol.* **17**, 5679-5687.

Cheah, K.S., Levy, A., Trainor, P.A., Wai, A.W., Kuffner, T., So, C.L. et al. (1995). Human COL2A1-directed SV40 T antigen expression in transgenic and chimeric mice results in abnormal skeletal development. *J. Cell Biol.* **128**, 223-237.

Chen, F. and Capecchi, M. R. (1997). Targeted mutations in hoxa-9 and hoxb-9 reveal synergistic interactions. *Dev. Biol.* **181**, 186-196.

Chen H., Rossier, C., Nakamura, Y., Lynn, A., Chakravarti, A. and Antonarakis, S. E. (1997). Cloning of a novel homeobox-containing gene, PKNOX1, and mapping to human chromosome 21q22.3. *Genomics* **41,** 193-200.

Colvin, J. S., Bohne, B. A., Harding, G. W., McEwen, D. G. and Ornitz, D. M. (1996). Skeletal overgrowth and deafness in mice lacking fibroblast growth factor receptor 3. *Nat. Genet.* **12**, 390-397.

Condie, B. G. and Capecchi, M. (1993). Mice homozygous for a targeted disruption of hoxd-3 (Hox-4.1) exhibit anterior transformations of the first and second cervical vertebrae, the atlas and the axis. *Development* **119**, 579-595.

Condie, B. G. and Capecchi, M. (1994). Mice with targeted disruptions in the paralogous genes hoxa-3 and hoxd-3 reveal synergistic interactions. *Nature* **370**, 304-307.

Couly, G., Grapin-Botton, A., Coltey, P. and Le Douarin, N. M. (1996). The regeneration of the cephalic neural crest, a problem revisited: the regenerating cells originate from the contralateral or from the anterior and posterior neural fold. *Development* **122**, 3393-3407.

Dear, N., Colledge, W. H., Carlton, M. B. L., Lavenir, I., Larson, T., Smith, A. J. H., Warren, A. J., Evans, J., Sofroniew, M. V. and Rabbitts, T. H.

(1995). The Hox11 gene is essential for cell survival during spleen development. *Development* **121**, 2909-2915.

Deng, C., Wynshaw-Boris, A., Zhou, F., Kuo, A. and Leder, P. (1996). Fibroblast growth factor receptor 3 is a negative regulator of bone growth. *Cell* **84**, 911-921.

Depew, M. J., Liu, J. K., Long, J. E., Presley, R., Meneses, J. J., Pedersen, R. A. and Rubenstein, J. L. (1999). Dlx5 regulates regional development of the branchial arches and sensory capsules. *Development* **126**, 3831-3846.

DiMartino, J., Selleri L., Traver D., Firpo, M., Rhee, J., Warnke, R., O'Gorman, S., Weissman, I. L. and Cleary, M. L. (2001). The Hox Cofactor and Proto-oncogene Pbx1 is required for maintenance of definitive hematopoiesis in the fetal liver. *Blood* (in press).

Duboule, D. (1995). Vertebrate Hox genes and proliferation: an alternative pathway to homeosis? *Curr. Opin. Genet. Dev.* **5**, 525-528.

Favier, B., Rijli, F. M., Fromental-Ramain, C., Fraulob, V., Chambon, P. and Dolle, P. (1996). Functional cooperation between the non-paralogous genes Hoxa-10 and Hoxd-11 in the developing forelimb and axial skeleton. *Development* **122**, 449-460.

Ferretti, E, Marshall, H., Popperl, H., Maconochie, M., Krumlauf, R. and Blasi, F. (2000). Segmental expression of Hoxb2 in r4 requires two separate sites that integrate cooperative interactions between Prep1, Pbx and Hox proteins. *Development* **127**, 155-166.

Fromental-Ramain C., Warot, X., Lakkaraju, S., Favier, B., Haack, H., Birling, C., Dierich, A., Dolle, P. and Chambon, P. (1996). Specific and redundant functions of the paralogous Hoxa-9 and Hoxd-9 genes in forelimb and axial skeleton patterning. *Development* **122**, 461-472.

Gavalas, A., Studer, M., Lumsden, A., Rijli, F. M., Krumlauf, R. and Chambon, P. (1998). Hoxa1 and Hoxb1 synergize in patterning the hindbrain, cranial nerves and second pharyngeal arch. *Development* **215**, 1123-1136.

Gendron-Maguire, M., Mallo, M., Zhang, M. and Gridley, T. (1993). Hoxa-2 mutant mice exhibit homeotic transformation of skeletal elements derived from cranial neural crest. *Cell* **75**, 1317-1331.

Goff, D. J. and Tabin, C. J. (1997). Analysis of Hox D13 and Hox D11 misexpression in chick limb buds reveals that Hox genes affect both bone condensation and growth. *Development* **124**, 627-636.

González-Crespo, S., Abu-Shaar, M., Torres, M., Martínez, A., Mann, R. S. and Morata, G. (1998). Antagonism between extradenticle function and Hedgehog signalling in the developing limb. *Nature* **394**, 196-200.

Hall, P. A., Levison, D. A., Woods, A. L., Yu, C. C., Kellock, D. B., Watkins, J. A., Barnes, D. M., Gillet, C. E., Camplejohn, R., Dover, R., Waseem, N. H. and Lane, D. P. (1990). PCNA immunolocalization in paraffin sections: an index of cell proliferation with evidence of deregulated expression in some neoplasms. *J. Pathol.* **162**, 285-294.

Huang, W., Chung, U.-I., Kronenberg, H. M. and de Crombrugghe, B. (2000). The chondrogenic transcription factor Sox9 is a target of signaling by the parathyroid hormone-related peptide in the growth plate of endochondral bones. *Proc. Natl. Acad. Sci. USA* **10**, 1073-1078.

Hunger, S. (1996). Chromosomal translocations involving the E2A gene in acute lymphoblastic leukemia: clinical features and molecular pathogenesis. *Blood* **15**, 1211-1224.

Ito, A., Nose, T., Takahashi, S. and Mori, Y. (1995). Cyclooxigenase inhibitors augment the production of pro-matrix metalloproteinase 9 (Progelatinase B) in rabbit chondrocytes. *FEBS Lett.* **360**, 75-79.

Jacobs, Y., Schnabel, C. A. and Cleary, M. L. (1999). Trimeric association of Hox and TALE homeodomain proteins mediates Hoxb2 hindbrain enhancer activity. *Mol. Cell. Biol.* **19**, 5134-5142.

Jonsson, J., Carlsson, L., Edlund, T. and Edlund, H. (1994). Insulin-promoter-factor 1 is required for pancreas development in mice. *Nature* **371**, 606-609.

Kamachi, Y., Uchikawa, M. and Kondoh, H. (2000). Pairing SOX off: with partners in the regulation of embryonic development. *Trends Genet.* **16,** 182-187

Kamps, M. P., Murre, C., Sun, X. H. and Baltimore, D. A. (1990). A new homeobox gene contributes the DNA binding domain of the t(1;19) translocation protein in pre-B ALL. *Cell* **60**, 547-555.

Karaplis, A. C., Luz, A., Glowacki, J., Bronson, R. T., Tybulewicz, V. L. J., Kronenberg, H. M. and Mulligan, R. C. (1994). Lethal skeletal dysplasia from targeted disruption of the parathyroid hormone-related peptide gene. *Genes Dev.* **8**, 277-289.

Karsenty, G. (1999). The genetic transformation of bone biology. *Genes Dev.* **13**, 3037-3051.

Knoepfler, P. S. and Kamps, M. P. (1995). The pentapeptide motif of Hox proteins is required for cooperative DNA binding with Pbx1, physically

contacts Pbx1, and enhances DNA binding by Pbx1. *Mol. Cell. Biol.* **15**, 5811-5819.

Knoepfler, P.S., Calvo, K.R., Chen, H., Antonarakis, S.E and Kamps, M. P. (1997). Meis1 and pKnox1 bind DNA cooperatively with Pbx1 utilizing an interaction surface disrupted in oncoprotein E2a-Pbx1. *Proc. Natl. Acad. Sci. USA* **94**, 14553-14558.

Kontges, G. and Lumsden, A. (1996). Rhombencephalic neural crest segmentation is preserved throughout craniofacial ontogeny. *Development* **122**, 3229-3242.

Krumlauf, R. (1994). Hox genes in vertebrate development. *Cell* **78**, 191-201.

Kwan, K. M., Pang, M. K. M., Zhou, S., Cowan, S. K., Kong, R. Y. C., Pfordte, T., Olsen, B.R., Sillence, D., Tam, P. P. L. and Cheah, K. S. E. (1997). Abnormal compartmentalization of cartilage matrix components in mice lacking collagen X: implications for function. *J. Cell Biol.* **136**, 459-471.

Labosky, P. A., Winnier, G. E., Jetton, T. L., Hargett, L., Ryan, A. K., Rosenfeld, M. G., Parlow, A. F. and Hogan, B. L. (1997). The winged helix gene, MF3, is required for normal development of the diencephalon and midbrain, postnatal growth and milk-ejection reflex. *Development* **124**, 1263-1274.

Lanske, B., Karaplis, A. C., Lee, K., Luz, A., Vortkamp, A., Pirro, A., Karperien, M., DefiLze, L. H. K., Ho, C., Mulligan, R. C., Abou Samra, A. B., Juppner, H., Segre, G. V. and Kronenberg, H. M. (1996). PTH/PTHrP receptor in early development and Indian hedgehog-regulated bone growth. *Science* **273**, 663-666.

Lawrence, H. J., Helgason, C. D., Savageau, G., Fong, S., Izon, D. J., Humphries, R. K. and Largman, C. (1997). Mice bearing a targeted interruption of the homeobox gene HOXA9 have defects in myeloid, erythroid, and lymphoid hematopiesis. *Blood* **89**, 1922-1930.

Lu, Q., Knoepfler, P. S., Scheele, J., Wright, D. D. and Kamps, M. P. (1995). Both Pbx1 and E2A-Pbx1 bind the DNA motif ATCAATCAA cooperatively with the products of multiple murine Hox genes, some of which are themselves oncogenes. *Mol. Cell. Biol.* **15**, 3786-3795.

Maconochie, M. K., Nonchev, S., Studer, M., Chan, S.-K., Pöpperl, H., Sham, M. H., Mann, R. S. and Krumlauf, R. (1997). Cross-regulation in the mouse HoxB complex: the expression of Hoxb2 in rhombomere 4 is regulated by Hoxb1. *Genes Dev.* **11**, 1885-1895.

Manley, N. R. and Capecchi, M. (1997). Hox group 3 paralogous genes act synergistically in the formation of somitic and neural crest-derived structures. *Dev. Biol.* **192**, 274-288.

Manley, N. R. and Capecchi, M. (1998). Hox group 3 paralogsregulate the development and migration of the thymus, thyroid and parathyroid glands. *Dev. Biol.* **195**, 1-15.

Mann, R. S. and Chan, S. K. (1996). Extra specificity from extradenticle: the partnership between HOX and PBX/EXD homeodomain proteins [published erratum appears in Trends Genet. 1996. Aug;12(8):328]. *Trends Genet.* **12**, 258-262.

McLeod, M. J. (1980). Differential staining of cartilage and bone in whole mouse fetuses by alcian blue and alizarin red S. *Teratology* **22**, 299-301.

Mercader, N., Leonardo, E., Aspiazu, N., Serrano, A., Morata, G., Martinez, A. and Torres, M. (1999). Conserved regulation of proximodistal limb axis development by Meis/Hth. *Nature* **402**, 425-429.

Monica, M., Galili, N., Nourse, J., Saltman, D. and Cleary, M. L. (1991). Pbx2 and Pbx3, new homeobox genes with extensive homology to the human proto-oncogene Pbx1. *Mol. Cell. Biol.* **11**, 6149-6157.

Moscow, J. J., Bullrich, F., Huebner, K., Daar, I. O. and Buchberg, A. M. (1995). Meis1, a PBX1-related homeobox gene involved in myeloid leukemia in BXH-2 mice. *Mol. Cell. Biol.* **15**, 5434-5443.

Nagase, H. (1998). Stromelysins 1 and 2. In *Matrix Metalloproteinases* (ed. W. C. Parks, and R. P. Mecham), pp. 43-84. San Diego: Academic Press.

Ng, L. J., Tam, P. P. and Cheah, K. S. (1993). Preferential expression of alternatively spliced mRNAs encoding type II procollagen with a cysteine-rich amino-propeptide in differentiating cartilage and nonchondrogenic tissues during early mouse development. *Dev. Biol.* **159**, 403-417.

Ng, L. J., Wheatley, S., Muscat, G. E., Conway Campbell, J., Bowles, J., Wright, E., Bell, D. M., Tam, P. P., Cheah, K. S. and Koopman, P. (1997). SOX9 binds DNA, activates transcription, and coexpresses with type II collagen during chondrogenesis in the mouse. *Dev. Biol.* **183**, 108-121.

Nourse, J., Mellentin, J. D., Galili, N., Wilkinson, J., Stanbridge, E., Smith, S. D. and Cleary, M. L. (1990). Chromosomal translocation t(1;19) results in synthesis of a homeobox fusion mRNA that codes for a potential chimeric transcription factor. *Cell* **60**, 535-545.

Nowakowski, R.S., Lewin, S.B. and Miller, M.W. (1989). Bromodeoxyuridine immunohistochemical determination of the length of the cell cycle and the DNA-synthetic phase for an anatomically defined population. *J. Neurocytol.* **18**, 311-318.

Offield, M. F., Jetton, T. L., Labosky, P. A., Ray, M., Stein, R. W., Magnuson, M.A., Hogan, B. L. and Wright, C. V. (1996). PDX-1 is required for pancreatic outgrowth and differentiation of the rostral duodenum. *Development* **122**, 983-995.

Olsen, B. R., Reginato, A. M. and Wang, W. (2000). Bone development. *Annu. Rev. Cell Dev. Biol.* **16**, 191-220.

Peers, B., Sharma, S., Johnson, T., Kamps, M. and Montminy, M. (1995). The pancreatic islet factor STF-1 binds cooperatively with Pbx to a regulatory element in the somatostatin promoter: importance of the FPWMK motif and of the homeodomain. *Mol. Cell. Biol.* **15**, 7091-7097.

Peifer, M. and Weischaus, E. (1990). Mutations in the *Drosophila* gene extradenticle affect the way specific homeo domain proteins regulate segmental identity. *Genes Dev.* **4**, 1209-1223.

Peltenburg, L. T. C. and Murre, C. (1996). Engrailed and Hox homeodomain proteins contain a related Pbx interaction motif that recognizes a common structure present in Pbx. *EMBO J.* **15,** 3385-3393.

Penkov, D., Tanaka, S., Di Rocco, G., Berthelsen, J., Blasi, F. and Ramirez, F. (2000). Cooperative interactions between PBX, PREP, and HOX proteins modulate the activity of the alpha 2(V) collagen (COL5A2) promoter. *J. Biol. Chem.* **275**, 16681-16689.

Phelan, M. L., Rambaldi, I. and Featherstone, M. S. (1995). Cooperative interactions between HOX and PBX proteins mediated by a conserved peptide motif. *Mol. Cell. Biol.* **15**, 3989-3997.

Popperl, H., Bienz, M., Studer, M., Chan, S.-K., Aparicio, S., Brenner, S., Mann, R. S. and Krumlauf, R. (1995). Segmental expression of Hoxb-1 is controlled by a highly conserved autoregulatory loop dependent upon exd/pbx. *Cell* **81**, 1031-1042.

Popperl, H., Rikhof, M. H., Chang, H., Haffter, P., Kimmel, C. B. and Moens, C. B. (2000). *Lazarus* is a novel *Pbx* gene that globally mediates Hox gene function in zebrafish. *Mol. Cell* **6**, 255-267.

Rauskolb, C., Peifer, M. and Wieschaus, E. (1993).extradenticle, a regulator of homeotic gene activity, is a homolog of the homeobox-containing human proto-oncogene pbx1. *Cell* **74**, 1101-1112.

Rijli, F. M., Mark, M., Lakkaraju, S., Dierich, A., Dolle, P. and Chambon, P. (1993). A homeotic transformation is generated in the rostral branchial region of the head by disruption of Hoxa2, which acts as a selector gene. *Cell* **75**,1333-1349.

Roberts, C. W. M., Shutter, J. R. and Korsmeyer, S. J. (1994). Hox11 controls the genesis of the spleen. *Nature* **368,** 747-749.

Roberts, V. J., van Dijk, M. A. and Murre, C. (1995). Localization of Pbx1 transcripts in developing rat embryos. *Mech. Dev*. **51**, 193-198.

Schnabel, C. A., Jacobs, Y. and Cleary, M. L. (2000). HoxA9-mediated immortalization of myeloid progenitors requires molecular interactions with TALE cofactors Pbx and Meis. *Oncogene* **19**, 608-616.

Schnabel, C., Selleri, L., Jacobs, Y., Warnke, R. and Cleary, M.L. (2001). Expression of Pbx1b during mammalian organogenesis. *Mech. Dev.* **100**, 131-135.

Shen, W. F., Chang, C. P., Rozenfeld, S., Sauvageau, G., Humphries, R. K., Lu, M., Lawrence, H. J., Cleary, M. L. and Largman, C. (1996). Hox homeodomain proteins exhibit selective complex stabilities with Pbx and DNA. *Nucleic Acids Res.* **24**, 898-906.

Shimamoto, T., Tang, Y., Naot, Y., Nardi, M., Brulet, P., Bieberich, C. J. and Takeshita, K. (1999). Hematopoietic progenitor cell abnormalities in Hoxc-8 null mutant mice. *J. Exp. Zool.* **283**, 186-193.

Sternlicht, M. D., Lochter, A., Sympson, C. J., Huey, B., Rougier, J. P., Gray, J. W., Pinkel, D., Bissell, M. J. and Werb, Z. (1999). The stromal proteinase MMP3/stromelysin-1 promotes mammary carcinogenesis. *Cell* **98**, 137-146.

St-Jacques, B., Hammerschmidt, M. and McMahon, A.P. (1999). Indian hedgehog signaling regulates proliferation and differentiation of chondrocytes and is essential for bone formation. *Genes Dev.* **13**, 2072-1223.

Swift, G. H., Liu, Y., Rose, S. D., Bischof, L. J., Steelman, S., Buchberg, A. M., Wright, C. V. and MacDonald, R. J. (1998). An endocrine-exocrine switch in the activity of the pancreatic homeodomain protein PDX1 through formation of a trimeric complex with PBX1b and MRG1 (MEIS2). *Mol. Cell. Biol.* **18,** 5109-5120.

Van Dijk, M. A. and Murre, C. (1994). extradenticle raises the DNA binding specificity of homeotic selector gene products. *Cell* **78**, 617-624.

Vogt, T. F and Duboule, D. (1999). Antagonists go out on a limb. *Cell* **99**, 563-566.

Vortkamp, A., Lee, K., Lanske, B., Segre, G. V., Kronenberg, H. M. and Tabin, C. J. (1996). Regulation of rate of cartilage differentiation by Indian hedgehog and PTH-related protein. *Science* **273**, 613-622.

Vu, T. H., Shipley, J. M., Bergers, G., Helms, J. A., Hanahan, D., Shapiro, S. D., Senior, R. M. and Werb, Z. (1998). MMP9/Gelatinase B is a key regulator of growth plate angiogenesis and apoptosis of hypertrophic chondrocytes. *Cell* **93**, 411-422.

Vu, T. H. and Werb, Z. (1998). Gelatinase B: structure, regulation, and function. In *Matrix Metalloproteinases* (ed. W. C. Parks, and R. P. Mecham), pp. 115-148. San Diego: Academic Press.

Wai, A. W. K., Ling, J. N., Watanabe, H., Yamada, Y., Tam, P. P. L. and Cheah, K. S. E. (1998). Disrupted expression of matrix genes in the growth plate of the mouse cartilage deficiency (cmd) mutant. *Dev. Genet.* **22**, 349-358.

Wilkinson, D. and Green, J. (1990). In *Postimplantation Mouse Embryos: A Practical Approach* (eds A. J. Copp, D. L. Cockcroft, and B. D. Hames), pp. 155-171. Oxford: IRL.

Wilkinson, D. (1992). In *In-situ Hybridization: A Practical Approach.* (ed D.G. Wilkinson), pp. 75-83. Oxford: IRL.

Wright, E., Hargrave, M. R., Christiansen, J., Cooper, L., Kun, J., Evans, T., Gangadharan, U., Greenfield, A. and Koopman, P. (1995). The Sry-related gene Sox-9 is expressed during chondrogenesis in mouse embryos. *Nat. Genet.* **9**, 15-20.

Yu, A. E., Murphy, A. N. and Stetler-Stevenson, W. G. (1998). 72-kDa gelatinase (Gelatinase A): structure, activation, regulation and substrate specifcity. In *Matrix Metalloproteinases* (ed. W. C. Parks, and R. P. Mecham), pp. 85-113. San Diego: Academic Press.

Yueh, Y. G., Gardner, D. P. and Kappen, C. (1998). Evidence for regulation of cartilage differentiation by the homeobox gene HoxC8. *Proc. Natl. Acad. Sci. USA* **95**, 9956-9961.

Zákány, J. and Duboule, D. (1999). Hox genes in digit development and evolution. *Cell Tissue Res.* **296**, 19-25.